We, the willing,
led by the unknowing
are doing the impossible
for the ungrateful.
We have done so much
for so long, with so little;
we are now qualified
to do anything
with nothing.

-1st semester 1st year linear algebra textbook. Credited to Konstantin Josef Jireček

Development and Prototyping of a Biologically Inspired Knee Prosthesis

by

Jacob Andrew Lufkin

B.Sc. Mechanical Engineering, University of New Brunswick, 2021

A Thesis Submitted in Partial Fulfillment
of the Requirements for the Degree of

Master of Science in Engineering

in the Graduate Academic Unit of Mechanical Engineering

Supervisors:	Chris McGibbon, PhD, Faculty of Kinesiology
	Juan Carretero, PhD, Dept. of Mechanical Engineering
Examining Board:	Rickey Dubay, PhD, Dept. of Mechanical Engineering, Chair
	Mohsen Mohammadi, PhD, Dept. of Mechanical Engineering
	Ed Biden, PhD, Dept. of Mechanical Engineering
	Wayne Albert, PhD, Faculty of Kinesiology

This thesis is accepted by the
Dean of Graduate Studies

THE UNIVERSITY OF NEW BRUNSWICK

October, 2024

ABSTRACT

A design for a biologically inspired knee prosthesis is presented. The design comes from using spring-driven devices in an antagonistic fashion to control both the position and stiffness of the knee joint. This work presents a proof-of-concept design that seeks to both develop an understanding of how to design and build a usable model and compare that physical model against a simulated model of the knee. The design was made in a pragmatic fashion and sources of error were mitigated during development. The final design following an intensive iterative design project allowed for quasi-static stiffness testing. The model was compared against simulated data. The model showed stiffening behavior and control over the position of the tibial component. It also showed a high amount of correlation to the simulated data. This holds promise for the future of the design, as it is proven to be feasible to build and simulations of optimized geometries can be trusted to yield valid data.

DEDICATION

This thesis is dedicated to my significant other, Kaitlin Taylor. Without her continued support, patience, and understanding, I would not have been able to complete the current work.

ACKNOWLEDGEMENTS

This work was not done singlehandedly. There are four people (besides supervisors – whose assistance goes without saying) whose contributions made an enormous impact on this work. First, Vince Boardman, who was always willing to listen and lend a helping hand when I needed to rationalize something, talk through a problem, or simply to chat. Next, Tony Guimond, without whom the physical prototype would not have taken shape. I am forever thankful for him allowing me to work in his shop and for fielding my design questions with patience and experience. Finally, my two lab-mates, Paul Sanford and Sage van der Laan. Paul, who has been by my side throughout my time at UNB, was always available to talk through problems of all sorts as we both progressed in our post-grad work. And without Sage, the testing of the apparatus would not have occurred. Sage was instrumental in creating valid testing procedures, and providing guidance in the data that would be necessary for the project going forward.

To these people, and to everyone who has lent guidance throughout the years of this project (Dylan Larter, Steve Blazeki, Kristel Desjardins, Jon Sensinger, Heather Daley, Dan Dafonseca), thank you.

Table of Contents

List of Tables

List of Figures

1. Introduction

1.1 Motivation

There is no greater machine than the human body. Through millions of years of evolution, the actions we perform as daily activities of living have been optimized and perfected to a subconscious level. The goal in the research, modelling, and designing of prostheses is to attempt to recreate the level of function and perfection exhibited by the human body. It is only natural, therefore, to use the body as inspiration for the design of prostheses. Biologically-inspired prostheses are not a novel concept, and in fact are very heavily researched in the field of biomedical engineering [1], [2], [3]. The challenge for researchers exists in finding ways to recreate the complexity of biological limbs, joints, muscles, *etc*. In this work, the human knee joint will be explored, and a biologically-inspired method for actuation, control, and stability is presented.

The field of prosthetics within biomedical engineering has been striving, since its inception, to allow persons with limb loss to restore function during activities of daily living. Specifically, the field of lower limb prostheses finds issues with patient satisfaction and acceptance by transtibial (below-knee) and transfemoral (above-knee) amputees [4]. Users of lower-extremity prosthesis have higher incidence of osteoarthritis and other joint related diseases in their residual limb, and the knee and hip joints of the intact limb [5]. The loss of primary function and the co-morbidities associated with using a prosthesis contribute to a high prevalence of depression and anxiety symptoms post-amputation [6].

It is therefore crucial for the amputee's mental and physical health that the prosthesis be as natural and intuitive as possible.

Currently, prostheses vary greatly depending on the level of complexity and price of the device. For knee prostheses, the complexity of devices ranges from simple passive mechanical joints to microprocessor-controlled joints, with knee motion prescribed by either a unicentric "hinge" or a polycentric stance-phase control mechanism [7]. Typically, the more advanced and complex a prosthesis is, the higher the cost to the user. This is problematic, as people with the same level of amputation can receive very different prostheses depending on their level of insurance or ability to pay out of pocket. Some of the most affordable knee prostheses are those with purely mechanical (non-microcontroller controlled) knee joints – typically broken down by the complexity of the mechanical linkage allowing for movement. The most simplistic knee joints approximate knee movement with a single hinge joint. While more affordable, they tend to increase activation of hip muscles of the residual limb to swing the leg forward, and can pose an increased fall risk if not used properly [8]. A step above the hinge knee is a locking four-bar knee, typically referred to as "stance-phase control" prosthesis. These devices are passive and rely on the individual's gait pattern to shift the center of rotation of the artificial joint to either lock the mechanism (for heel strike) or allow the mechanism to swing (for swing phase) [9]. Most notably, the joint center of rotation dictated by these prostheses is non-anatomical by design, which means that the user must adapt to the prosthesis in order to control its movement.

Passive mechanical knee prostheses, whether single axis friction hinge or four-bar stance-phase locking mechanisms (and up to and beyond eight-bar mechanisms seen in academia, not typically seen in practical use [10]) all seek to provide stability and promote walking function. One issue with passive stance-phase locking mechanisms is that they often require substantial clinical rehabilitation to be able to use effectively. In fact, in the definition of the most commonly used stance-phase controlled mechanism (the "Radcliffe" knee [9]), it is stated that the ability to control the motion and stability of the knee depends on the physical ability of the amputee. This is a common issue that people with lower-extremity amputation face, as they must intentionally change their gait to adapt to their prosthesis. Other than limited mechanical adjustments for body size, there is little option for the prosthesis to adapt to the individual. Consequently, some individuals will opt to either not use the prosthesis, or they will develop a deviated gait, for instance compensating for the lack of natural motion in the limb by "swinging" the leg using the hip [5]. This can lead to physical and psychological disabilities, as detailed above.

One step above the passive-mechanical prosthesis is a microprocessor-controlled knee. A common microprocessor-controlled knee used in analysis against passive-mechanical knees is the Ottobock C-Leg [7], [8], [11]. Microprocessor-controlled knees can monitor and control the stance and swing phases of gait but do not provide any external power to the joint. While MPK devices have been shown to increase user quality of life, decrease self-reported falls, and increase walking speed over a traditional passive-mechanical knee [11], they are only attainable at a much higher price to the individual. Even with microprocessor-controlled knee joints, stepping asymmetries persist [12] and there still

exists the increased risk of osteoarthritis in the in-tact limb due to non-normal gait patterns [13].

Another issue with traditional passive prostheses is the lack of active power that can be drawn from a natural knee joint. Active power comes from the knee joint when it needs to self-actuate, as opposed to simply transferring power during gait. This can be exhibited during tasks like getting up from a chair or walking upstairs, but also occurs during walking as well, albeit to a lesser extent. The solution to this problem is a powered knee prosthesis. Currently, however, there are a limited number of commercial knee prostheses that can provide power to the joint, such as the Össur Power knee from Össur and the IntelLeg Knee from Reboocon Bionics [7]. These prostheses carry a larger price point than the passive microprocessor-controlled knees discussed above, and therefore less often used [8].

One reason for the increased price point of microprocessor-controlled knees and power knees are the complexity and power requirements needed from the device's motor(s). One helpful feature of implementing an antagonistically driven variable stiffness actuator (VSA) as opposed to a rigid actuator seen in conventional active prostheses is the potential for energy storage and timed-release capabilities of the spring elements of an agonist-antagonist VSA. In theory, the addition of mechanical energy storage/release enabled by the VSA should help to reduce the motor size and power requirements and help to decrease cost. Characterization of energy storage and motor sizing is, however, beyond the scope of this proof-of-concept work.

A challenge in the field of lower extremity prostheses is developing an inexpensive prosthesis that is capable of enabling an energy efficient and safe gait pattern. The biological knee can be seen as an inspiration for these criteria, as it excels at regulating power that flows through it [14]. The knee joint actuators (muscles) can regulate the work done either by or on the joint by controlling the energy transferred between segments. The analysis of mechanical energy transfer between leg segments through a prosthesis is beyond the scope of this work. However, the usage of devices that are capable of storing mechanical energy in the form of springs, combined with a precise control scheme, may be a way to reduce burden on the ipsilateral hip and contralateral limb, and improve the metabolic efficiency of walking with an above-knee prosthesis.

The concept of biologically inspired prosthetics is not new. By using the biological knee joint as inspiration, an area of prosthetics research that investigates the concept of using springs that act as biological muscles began in the early 2000's [15], [16]. The most important advancement made from this idea was using springs in an agonist-antagonist setup, just like the biological quadriceps/hamstrings.

As shown in [15], [16] using linear spring components allowed for energy storage, reducing the total energy cost of using the prosthesis. Most of these devices, termed variable stiffness actuator-powered prostheses (VSA-powered prostheses) are only used for research purposes and have not made their way into the general market. This is due to the high complexity and relative novelty of this method of actuation and control. Furthermore, as detailed by English & Russel in their landmark 1999 paper that introduced the concept of

agonist-antagonist VSA, there are significant limitations to utilizing linear spring actuators for stiffness control [17]. If a prosthesis were created that could use the biologically-inspired agonist-antagonist control theory, not be affected by spring actuator range of motion, while also being constrained by the pillars of cost effectiveness, energy efficiency, and natural motion, it may be able to solve some of the issues that prosthesis users face today.

The current work seeks to advance the field towards these goals by researching methods of enabling mechanical energy storage and transfer via agonist-antagonist torsional or spiral springs. At the same time, it seeks to explore the how kinematic constraints of the natural knee may influence performance of a future agonist-antagonist VSA (complete with motors and controllers).

1.2 Contribution towards gap in field

Agonist-antagonist driven VSAs are lacking in the field of above-knee knee prostheses. The concepts of replicating muscle activation and mimicking biological geometries are promising in both their simplicity of understanding the high-level concepts, and their ability to control the knee; however, to date there are no commercial agonist-antagonist VSA available to amputees. This work made a step towards being able to design a biologically inspired powered knee prosthesis. The creation of this proof-of-concept device allows for confidence to be placed in simulated versions of the device in the future and ironed out issues with physically creating a biologically inspired model. Proving that this biologically inspired design can be manufactured will allow for further iterations to venture

securely into the next steps of design optimization and development of the motor controller architecture required to constitute a functioning VSA that can be tested with human subjects.

1.3 Aims and objectives

There were two major aims of this project. First, the development of the physical device to verify that it would be able to modify stiffness and position based on inputs to spring-driven devices. Second, this model serves as a physical verification of a mathematical (computer) simulation that is based entirely on fundamental mechanical engineering principles and equations of motion. Correlation between the mathematical model outputs and outputs from the physical model gives confidence to the simulation and enables further experimentation and optimization using the mathematical model.

- Fabricate a scale model of the proposed mechanism and ensure desired range of motion (ROM) is attainable.
- Fabricate a spring-driven device capable of providing a variable amount of torque, based on initial spring pretension, to independently modulate stiffness of either flexor or extensor actuators.
- Design a testing apparatus that incorporates a spring-driven device for use in measuring the position and stiffness of the knee joint.
- Evaluate the ability of the knee joint to move through its ROM and stiffen based on inputs to the spring-driven devices.
- Compare the stiffening abilities of the physical model to an existing mathematical model and determine if there is a correlation.

2. Background

2.1 Outline

The interdisciplinary and multi-faceted nature of this design requires background in fields such as anatomy, biomechanics, kinematics, variable stiffness actuators (VSAs), and computer aided design (CAD). Anatomy is relevant to this project due to the nature of the novel design, which utilizes the biological anterior cruciate ligament (ACL) – posterior cruciate ligament (PCL) configuration. It is necessary to understand the entire anatomy of the knee, however, as some design decisions are based on the replication or purposeful neglection of biological systems. Biomechanics is a valuable field as it pertains to the forces involved with human movement, which provides insight to how the VSA system should be designed. A review of the biomechanics of the lower limbs as related to healthy human walking (gait) will be explored to characterize the forces and moment seen at the knee. A kinematic overview of the trajectory of the design will highlight key differences between the current design and those described in the work done by Radcliffe describing traditional open stance phase knee mechanisms [9]. VSAs will serve as the actuators of our design and require an explanation as to why they are used to mimic human biology. Finally, numerous CAD models and a physical prototype were developed and tested by the author prior to commencing formal thesis studies. Stepping through this work will provide background and insight into the evolution of this project, leading to the current methodological approach employed in this thesis.

2.2 Anatomy and biomechanics

2.2.1 Basic anatomy of the knee

The knee joint is one of the most important biomechanical systems in the human body, which then implies the loss of the knee to be a substantial impairment. More than just a method of controlling the distal end of the legs, the knee joint is a complex system that deals with stability, gait pattern, and gait efficiency. Moving distally, the knee sits at the end of the femur, with the proximal attachments of the anterior and posterior cruciate ligaments. These cruciate ligaments are of importance to this work, as they guide the trajectory of the tibia about the femur.

The knee joint is often referred to as a hinge joint, but its actual motion is more complicated. As shown in [18], the path of the knee joint can be approximated by the motion of a four-bar mechanism comprised of the anterior cruciate ligament, posterior cruciate ligament, and the lengths between their corresponding attachment sites on the femur and tibia. These attachments are shown in Figure 1. As these ligaments are unable to resist compression, the assumption that they can be modeled as isometric links comes from the fact that the mating tibial plateau and femoral condyles (behind the overlaid links in Figure 1) remain in contact, and act to keep the ligaments taught throughout the entire range of motion of the joint. The ACL-PCL complex characterizes the knee's rolling-sliding motion when viewed as isometric links of a four-bar mechanism, and therefore establishes an instant center of rotation (ICR) at the location of the crossed links. In this document, it is assumed that because these links form a four-bar whose motion

characterizes the motion of the knee mechanism [19], that this created ICR is also the center of rotation of the biological knee.

In this work, we are accepting the hypothesis that the ACL-PCL complex has a secondary function (secondary to constraining anterior-posterior movement of the tibia with respect to the femur) to constrain the movement profile of the tibia's rotation/translation about the femur. This four-bar mechanism and its implications in the position analysis of the knee joint has been researched [19]. The movement profile of this four-bar mechanism allows a model knee to have a rolling-and-sliding effect during flexion, similar to that of a biological knee.

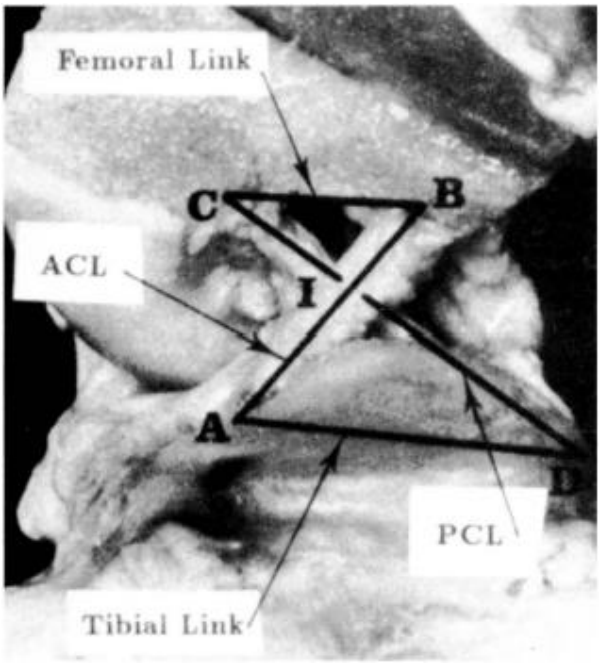

Figure 1: Four bar mechanism inside of the knee joint [19]

The knee joint is actuated by the surrounding muscles of the quadricep, hamstring, and gastrocnemius. These muscles work together to both actuate the knee in active flexion and extension and to provide stability. Stability occurs due to the tensing of the muscles on the respective ligaments and tendons of the knee joint and eliminating any laxity that may exist [20]. The cooperation of the muscles allows for static and dynamic stability of the joint.

2.2.2 Lower limb biomechanics

A study into the biomechanics of the lower limbs and their components is necessary to understand the joint angles, moments, and forces that will be applied to the proposed prosthesis. Biomechanics is defined as the application of mechanical principles to living organisms such as humans, and it plays an important part in the understanding of the principles of human motion [21]. In the context of a knee prosthesis, the biomechanics analysis will primarily focus on the forces and moments being placed on the knee throughout gait.

The human gait cycle is one of the most heavily studied and important parts of functional biomechanics [22]. A disruption to the body's normal gait cycle can have serious impacts on energy expenditure during walking and can lead to joint-related injuries if abnormal gait is not addressed. Therefore, when designing a knee prosthesis that seeks to restore a normal gait cycle, it is important to understand how human ambulation is performed.

The human gait cycle is defined as the cycle of heel strike to heel strike of the same foot. The gait cycle can be broken up into two distinct intuitive sections – stance phase and swing phase. Stance phase, defined as the percentage of the gait cycle where only one leg is in contact with the ground, makes up roughly 60% of the gait cycle. Swing phase, defined as the percentage of the gait cycle where the leg is swinging from toe-off to heel strike, makes up the remaining 40% [22]. Each section can be broken up into smaller subsections, which define markers used to identify healthy gait.

In stance phase, 5 indicators can be identified: initial contact, loading response, mid stance, terminal stance, and pre-swing. These markers define the limb's ability to accept the weight of the body and conserve forward momentum to swing the upper body forward. This leads to the "inverted pendulum" theory of human gait, where the swing phase of gait can be approximated as an inverted pendulum – rotation point on ground, mass is body. From the perspective of knee prosthesis design, it is important that the knee be sufficiently stiff during the stance phase of gait to allow the body's forward momentum to transition over the grounded limb. Here, the knee is not needed to be a highly mobile joint, but a stabilizing force within the leg using surrounding muscles.

In swing phase, 3 indicators can be identified: initial swing, mid swing, and terminal swing. The purpose of the swing phase of gait is to safely move the limb into position to begin weight acceptance. This mainly involves advancing the limb forward and ensuring that the toe does not drag, or else a fall could occur. In the first identifier of swing phase, the knee

plays a large part in limb advancement, as knee flexion during the initial swing climbs to 60 degrees which is the highest in the gait cycle.

2.3 Kinematics

The movement of the knee in the sagittal plane can be approximated by using a four-bar mechanism, as shown in Figure 2. For a kinematic analysis, a rigid crossed four-bar mechanism will be analyzed. The knee has a range of motion from -5 degrees (slightly past full extension-hyperextension) to roughly 140 degrees (full flexion). Therefore, the crossed four-bar mechanism must have its extreme angles at 0 and 140 degrees. In the biological knee, the ACL and PCL ligaments are defined by their attachment points on the tibial plateau. The ACL attaches anteriorly to the tibia and travels posteriorly to attach to the posterior femoral notch, and the PCL attaches posteriorly to the tibia and travels anteriorly to attach to the anterior femoral notch. During motion, the ACL inclines towards the tibia and away from the femur with increasing flexion, and the PCL inclines away from the tibia and towards the femur [19]. The movement of the linkages corresponding to the ACL, PCL, and femoral contact site are described moving relative to the tibial attachment site is shown in Figure 2. The link lengths used in the modelling of the four-bar mechanism used in this thesis work comes from work done by Bradley *et al.* [23]. Link lengths, shown in Appendix A, were taken from the dimensions of this “linkage” in four cadaver knees using radiographic measuring techniques.

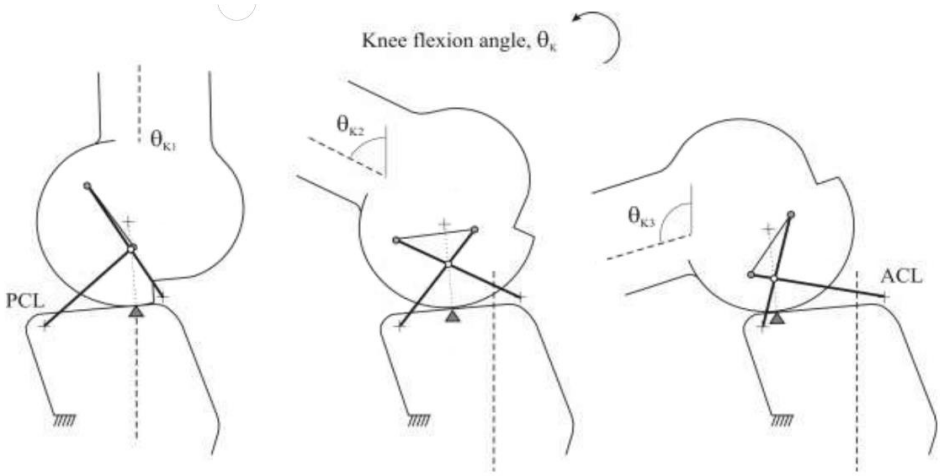

Figure 2: Positions of the four-bar mechanism at 0, 70, and 140 degrees of flexion [19]

Four-bar ICR

A conversation about Instant Centers of Rotation (ICRs), also known as Centers of Rotation (CORs), should be had as they are important to the stability of prosthetic knee joints, and a critical part of the crossed four-bar geometry discussed above. The most commonly seen four-bar mechanism in prostheses is an open four-bar, which can be seen opposed to a crossed four-bar in Figure 3.

All moving bodies can be examined as moving relative to some reference. Isolating one link of a four-bar mechanism, it can be simple to see that if it is fixed to a revolute joint, the body is rotating around that joint. This thinking can be expanded to view any bodies moving relative to one another as them rotating around some specific point – the ICR.

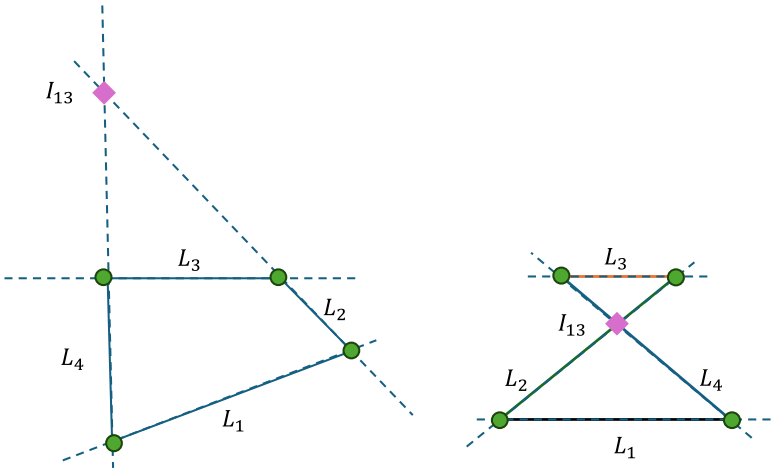

Figure 3: Open four-bar mechanism (left) vs. crossed four-bar mechanism (right), with relevant ICR highlighted

A four-bar mechanism expands this thought process and forces the analysist to consider what happens to ICRs of multiple planar bodies rotating relative to one another. The Kennedy-Arnholdt theorem holds that if three bodies are in relative planar motion (L_2, L_3, L_4), there are three ICRs (one for each pair of bodies - I_{23}, I_{24}, I_{34}. Further, these three ICRs are collinear. This is shown graphically for a general case, then for a crossed four-bar in Figure 4.

At any point in the movement of the mechanism, it is shown in [19] that the COR exists within the envelope of the four-bar linkage. This is shown graphically in Figure 5. This crossed structure of the four-bar mechanism differs from the common method of polycentric four-bar knees described by Radcliffe [9]. Radcliffe, and subsequent "open" four bar designs have the COR move outside the profile of the knee joint. Initially, the

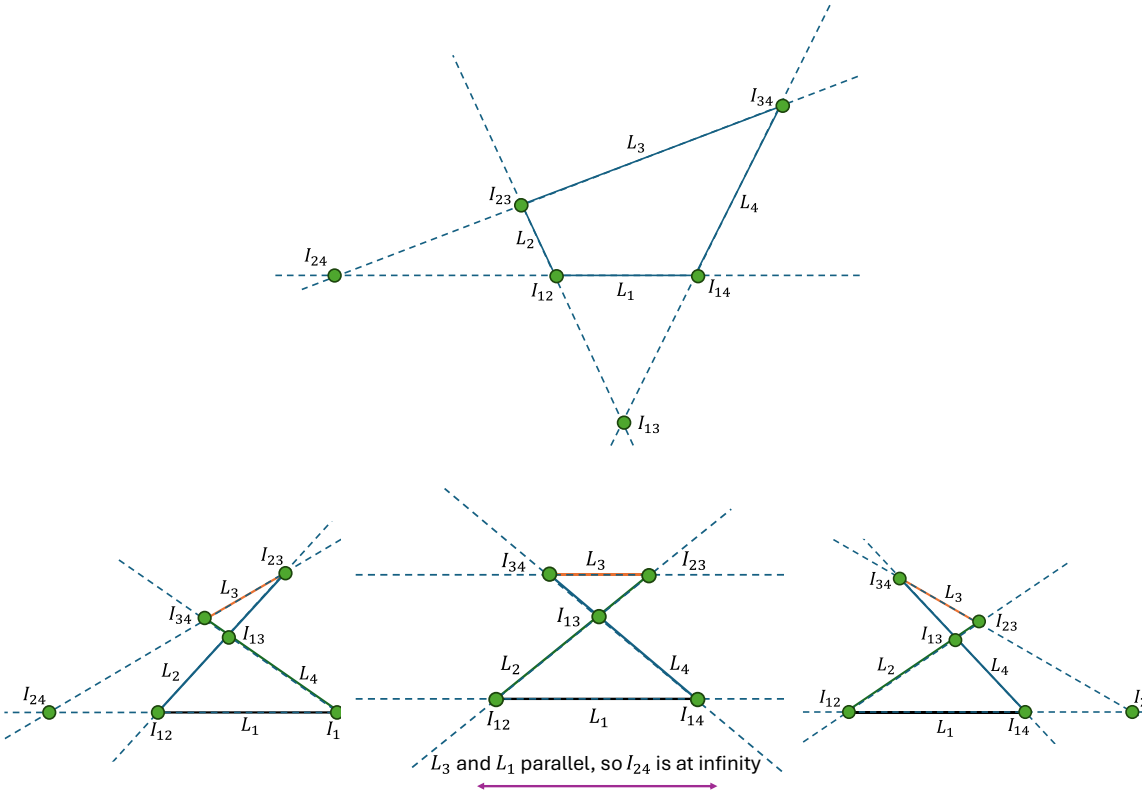

Figure 4: a (top): General four-bar mechanism with ICRs shown. b (bottom left): ICR representations of the crossed four bar in a left-facing orientation. c (bottom middle): ICR representations of the crossed four bar in a parallel orientation. d (bottom right): ICR representations of the crossed four bar in a right-facing orientation

COR is placed behind the line of loading in the leg (imaginary line stemming from heel and traveling up the leg), which increases the stability of the joint [9]. Subsequently at toe-off, the COR is in front of the loading line (this time from the toe, travelling up the leg), which is necessary for knee flexion [9]. For this process to happen such that a normal gait is achieved, effort must be exerted by the prosthesis wearer to shift the COR. In the crossed

four-bar mechanism, as in the biological knee, the COR does not move as substantially as in the Radcliffe knee. An advantage of this minimal movement of the COR is the maximization of internal moment arms needed to reverse direction of the joint. For example, in deep flexion, the moment arm of the quadricep mechanism is maximized in order to have the ability to change direction of the joint.

The optimal placement of the COR of knee prostheses is debatable, as the evidence is indirect in support of the crossed four-bar theory. It has been seen that the Radcliffe knee joint requires effort and training to shift the COR into advantageous positions, and even with training, bone related diseases such as osteoporosis are prevalent [5], [9]. Therefore, a prosthesis that by default has the COR in a natural position and ensures stability through an external system (VSA) that mimics the muscles could prove more optimal than the standard Radcliffe knee.

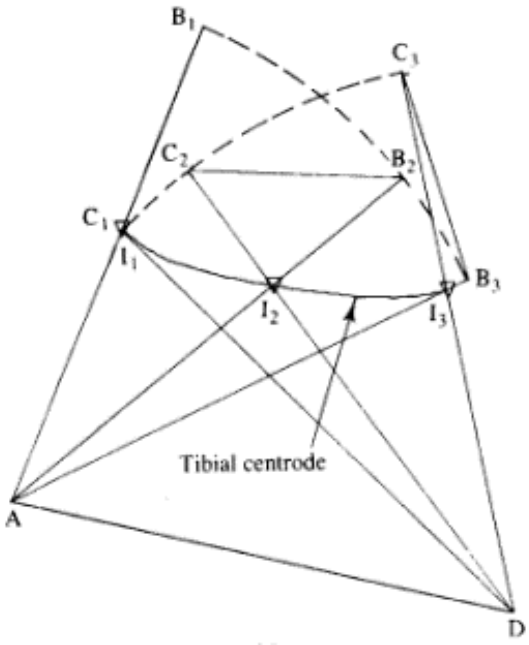

Figure 5: Center of rotation during travel of the four-bar mechanism [19]

The knee is a complex mechanism with one function being to transfer energy between the ankle joint and the hip joint during gait. The relevant anatomy of the knee has been discussed above. The knee, as most other joints in the body, is controlled via agonist antagonist muscles to ensure independent control over the joint. This antagonistic design is replicated in biomedical engineering by variable stiffness actuators and clever control schemes. The development of the control schemes necessary to produce a functioning VSA are beyond the scope of this work. However, it is worth noting that in the future work of this project, motor tuning and instantaneous stiffness control based on spring positioning would be able to render a range of stiffnesses.

2.4 Variable stiffness actuation

2.4.1 Concept

Variable stiffness actuators have been introduced into the field of biomedical engineering for their wide range of applications in replicating human movement. In essence, a VSA replaces a common rigid actuator by introducing a mechanical element between the actuator and the environment to conserve mechanical energy or change how the actuator is interacting with the world. These mechanical components can vary, from springs to flywheels, and for the purpose of this experiment the spring will be used as a mechanical element. An example of a VSA using springs in an agonist-antagonistic manner is shown below.

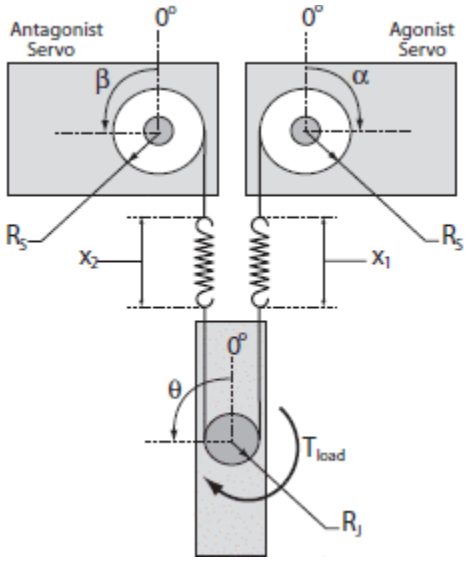

Figure 6: Example of an antagonistic setup for joint control [16]

A variable stiffness actuator can be used for biomedical purposes in numerous case-specific applications, but five common uses [24] are:

1. Shock absorbing,

2. Stiffness variation with constant load,
3. Stiffness variation at constant position,
4. Cyclic movements, and
5. Explosive movements.

This project highlights the second and third uses, being stiffness variation under load and during a constant position. The muscles of the body are able to change the stiffness of any given joint by altering their corresponding antagonistic muscle contraction/relaxation. For example, a forearm can remain at 90 degrees to the body while having a constant load applied at the hand and can also keep that position if more loads were to be applied. It should also be noted that these elements cannot be easily disentangled, as knee function inherently allows for shock absorbing, cyclic movements, and explosive movements. These are seen, for this project, as byproducts of a well-designed VSA that has full control over stiffness variation both at a constant load and constant position.

VSAs are an advancement on simplistic series-elastic actuator design. The use of a VSA allows for the control of both position and stiffness of the driven joint. This is analogous to most joints in the human body. Stiffness and position control for these actuators can be broken into two categories: agonist-antagonistic designs where two motors control one spring each, which actuates the terminal link, and serial designs where one motor controls the stiffness and one controls the position [25]. For this project, the former is considered. An agonist-antagonistic design is shown in Figure 6.

Numerous VSA-controlled devises exist for uses such as soft robotics, where robot-human interaction is necessary, and when robots need some sort of active compliance [24]. The field of prosthetic control with a VSA device is natural then, as prostheses are defined by their interactions with and through the human body. Using a VSA to control a knee prosthesis allows for the actuation of the knee joint in a biologically inspired fashion and has the potential for decreasing energy expenditure when compared to traditional powered or passive prostheses (for instance, the AAAKP as shown by Martinez-Villalpando *et al*. [26]).

While performing tasks associated with environmental hazards (stairs, hills, *etc*.) is possible with both a passive knee and microprocessor-controlled knees, data is uncertain of whether a microprocessor improves the ease at which these tasks are performed [13]. Therefore, it is likely that with both types of prostheses a non-natural method is used to perform these tasks to make up for the fact that no positive work can be done by the knee joint. An advantage that can be seen from the implementation of VSA control is the ability to provide net positive work from the knee joint. This, in turn, would help to complete tasks seen as hazards, such as stair climbing.

2.5 Design concept

2.5.1 Initial concept

This project has been ongoing for several years now, and this author has contributed since the summer of 2018. Initially, the proposed work was to be an antagonistically controlled

"rigid" actuator. The motivation for the work came from the observation that the position of a prosthesis could be controlled by two motors acting as the muscles controlling the knee joint. These motors would control pulleys that would wrap/unwrap cables or belts to pull the tibia about the distal end of the femur. The motion of the tibia, instead of being a simple hinge, could be guided by a biologically-inspired four-bar mechanism, like that seen in the 1989 paper by O'Connor *et al*. [19]. This concept would actively move both the extensor and flexor pulleys to maintain tension on the tibial component.

2.5.2 Design history

As described previously, the initial design prototype was a rigid actuator design focused on the movement profile of the knee prosthesis and looked to verify if the design was feasible. The kinematics of the crossed four-bar mechanism that serves as the knee joint were performed by McGibbon *et al.* [27] and the initial physical model was created in 2018 to simply visualize the movement of the model. At the end of the first summer of work on the model, the following CAD model (Figure 7) was created of the physical device with a rigid drive train to verify the joint could flex and extend while maintaining tension of the extensor and flexor actuator cables.

The following summer, work on the project continued, with a larger scaled up version of the knee being printed to test actuation methods. The actuation of the knee was performed by a gear train connected to pulley wheels that would turn and actuate the joint. A 3D printed version of this can be seen in Figure 8.

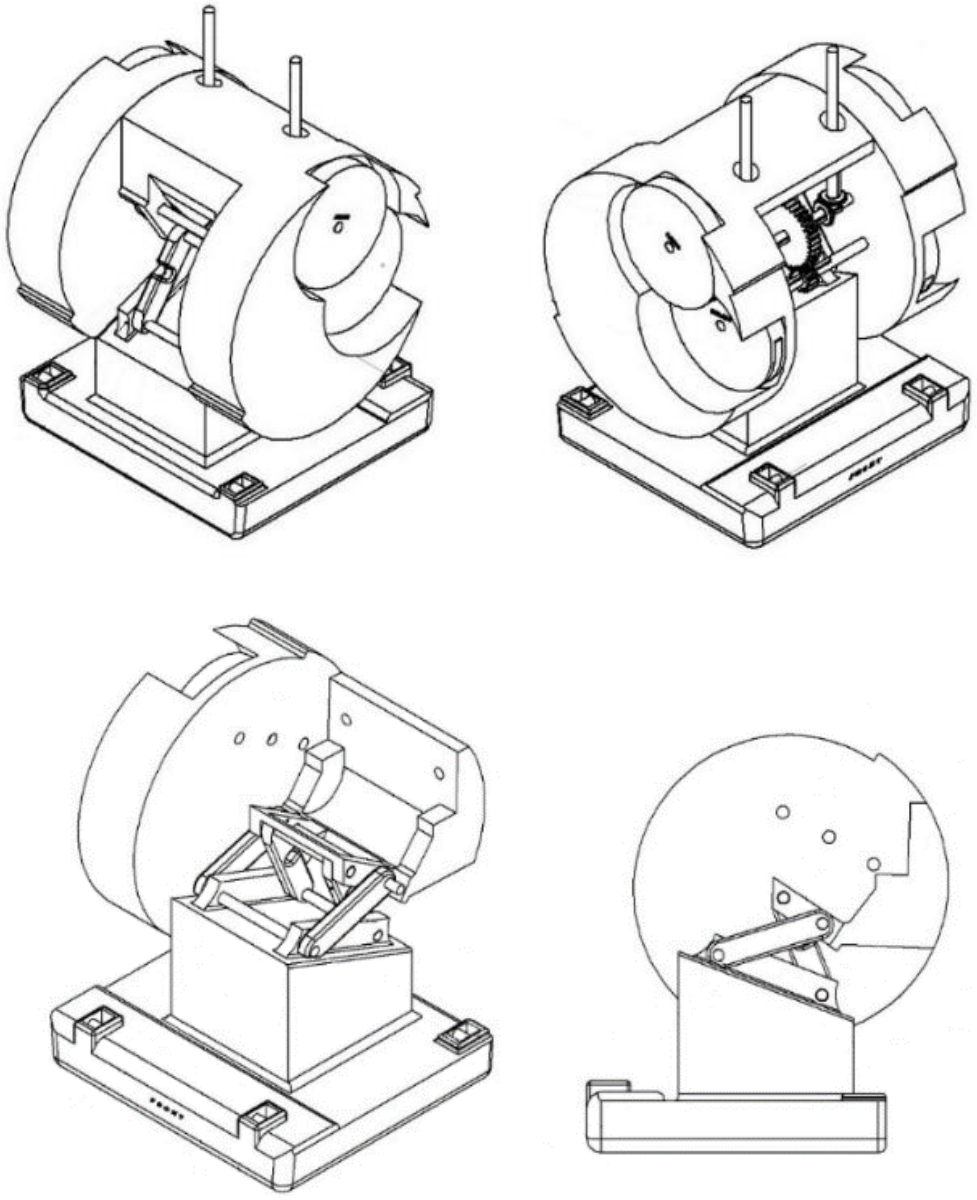

Figure 7: Oversized knee CAD model. Shown in a (top) with both sides to show pulley locations and in b (bottom) to reveal the four-bar.

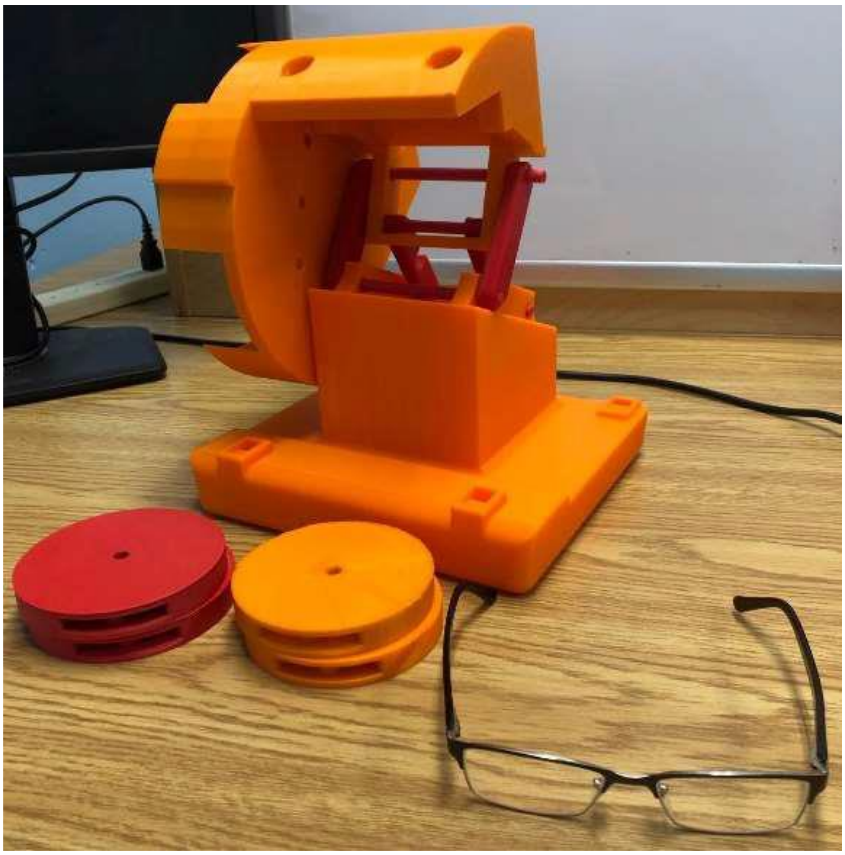

Figure 8: Printed version of the oversized knee model (glasses for reference)

This design model allowed for the placement of gears inside of the body of the model and to be driven externally. This model served to prove that the concept of a gear and pulley system could actuate the joint. The gears were implemented into this design as shown in Figure 9. When turned, the top rods would actuate the pulley wheels, which would cause the tibial component (bottom) to rotate about the femur in the path predetermined by the four-bar mechanism.

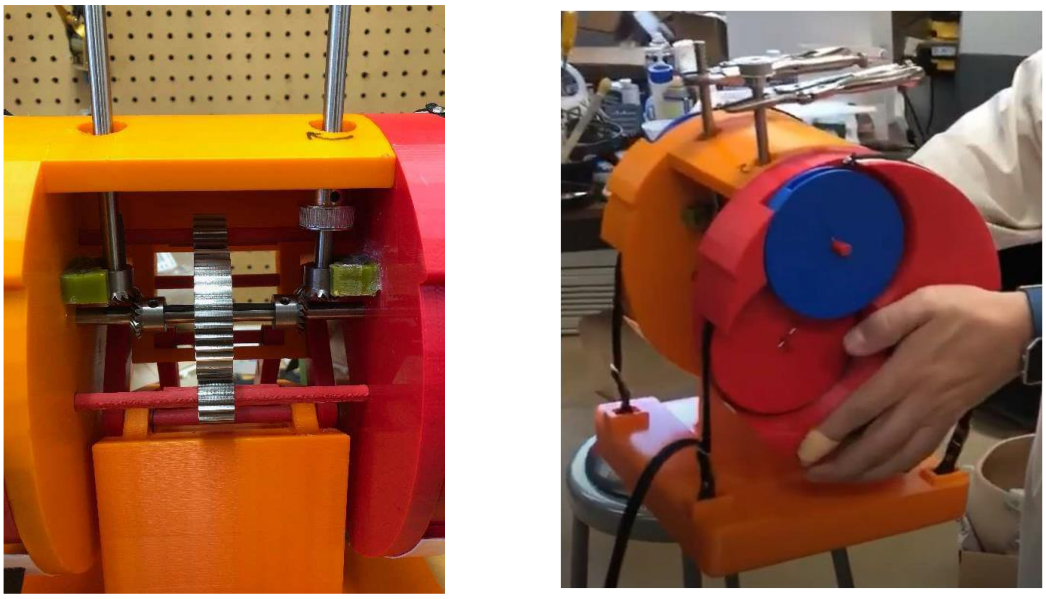

Figure 9: Printed version of oversized knee with direct-drive mechanism in place. 9a (left) 9b (right).

Further models of the mechanism would be extended to be able to drive the pulley wheels using a spring driven actuator (this project).

One notable change from the previous iterations of this project is the physical four-bar being used for actuation. Using traditional straight links poses an issue for a crossed four-bar mechanism. Due to the geometry of the tibial components and the need for rigidity in the actuation of the knee, all revolute joints needed to be fixed on either side of the four-bar. This means there would be rods passing through all joints, which can be seen in Figure 5 as points B and C. Using straight links would essentially lock the mechanism as any movement of the tibia would cause one of the connecting rods to come into contact with one of the crossed linkages. This problem was alleviated by using curved bars for the

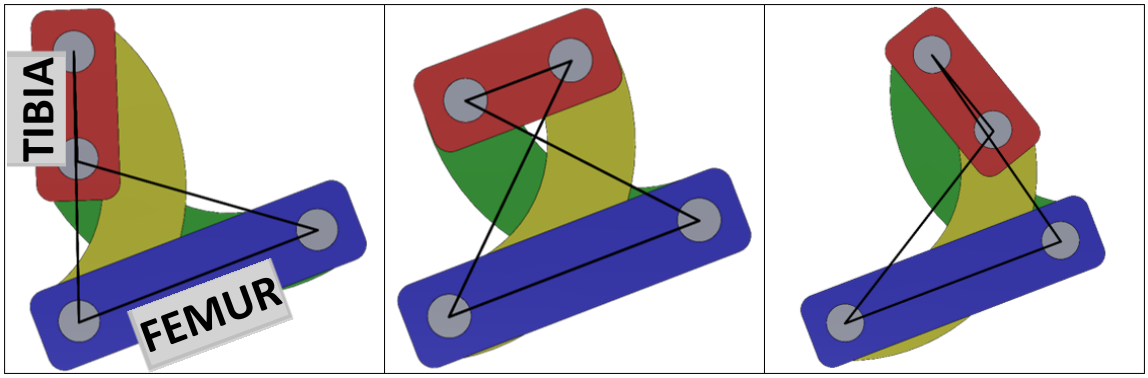

Figure 10: Detail of crossed four-bar linkage with curved members

crossing links. The revolute joints at the end of these bars remained the same length apart to keep the kinematic analysis valid. This is shown in Figure 10. Figure 10 shows the mechanism in the conventional four-bar orientation with the ground link on the bottom. This means that it is upside-down from the body's tibio-femoral interface. Also note that the "tibia" and "femur" links represent the attachment sites/plateaus on both bones.

2.6 Literature review

Variable stiffness actuators (VSA's) are robust devices that are being discovered as an energy efficient, biologically inspired way to actuate complex components. VSAs take their inspiration from multiple places, for example the antagonistic muscle control exhibited by the body, but also the need for safe human-robot interaction. Although the research in VSAs has greatly increased over the past 8 years, the original concept of an actuator coupled with some degree of compliance dates to around 1979. In N. Hogan's 1979 publication [28], he talks of the reason for the body's co-contraction and how it can influence the overall stiffness of an actuated joint. This work leads into Hogan's multi-part publication in 1984-1985 on impedance control, and its applications in robotic

manipulation [29]. This work undoubtedly led to further publications on variable impedance and series elasticity, such as the 1995 publication simply titled "Series Elastic Actuators" [30]. In [15], Laurin-Kovitz *et al*. refers to a simplistic variable stiffness device as having programmable passive impedance (PPI), which is the ability to control the amount of compliance in an actuator mechanism. Due to the nature of the field and general language used, this device included an adjustable damper and an adjustable spring. Therefore, this categorizes the device into the field of variable impedance actuators. This is a distinction that will become important as the field progresses into the 21st century as a considerable amount of research (discussed below) focuses solely on springs and not dampers to provide variable impedance.

In 1999, English and Russell [17] proposed that the recent investigations into variable stiffness actuators may be beneficial in the field of prosthetic limbs. In their paper, they look into the stiffness displacement problem of a joint antagonistically actuated by two linear springs. They found that to decouple the joint stiffness from deflection, the individual antagonistic springs must have a non-linear force profile. This is only shown mathematically in their paper. However, in 2005, Migliore *et al*. [16] proved physically that springs can be used in an antagonistic set-up to demonstrate simultaneous control of both joint angle and stiffness. Further, linear springs were used in this set-up. This was only possible due to the experimental set-up allowing for specifiable force-length relationships (producing non-linear force profiles). Migliore *et al*. use of linear springs validated a concern brought up in the English and Russel paper – the fact that size and spring deflections would play a part in determining the range of stiffnesses that can be

rendered. By replacing the linear springs with spiral springs that would be able to change their neutral position without needing to consider spatial accommodations, the range of stiffnesses that are able to be rendered should increase.

Energy efficiency has been mentioned by Migliore and English & Russell, but other than acting as a motivation no work was put into finding what energy conservation could be achieved with variable stiffness actuators. In 2008, Martinez-Villalpando *et al*. [2] proposed that the energy efficiency mentioned by the aforementioned authors could be used to the benefit of those suffering from lower limb loss. This was the motivation behind the agonist-antagonist active knee prosthesis (AAAKP), which (as the name suggests) uses an antagonistic spring set-up as defined by Migliore *et al*. and was made into a physical prototype. This study only utilized a simulation model of the prototype, but the authors claimed that it would reduce the total metabolic cost of overground walking for transfemoral amputees. This theory was tested in 2011 [26] by the same group when their prototype AAAKP was compared with an Ottobock C-Leg prosthesis. With trials on both able-bodied and amputee subjects, they were able to determine a significant decrease in metabolic cost and increase in self-selected walking speed. With this result, the benefit of a variable stiffness actuator implemented into a prosthesis began to be realized as an increasingly viable area of study, which spawned lots of inventive and interesting VSAs.

In 2012, Schuy *et al*. [31] first described using torsional springs in a variable stiffness configuration for biomedical purposes. Their device, which was called a VTS concept (variable torsional stiffness), performed just as well as other adjustable stiffness concepts

in terms of power consumption. The paper concludes with the authors recommending further work in implementing torsional stiffness control in biomechanical applications, even recommending an active knee prosthesis with this device be pursued. In search of an efficient way to return the energy to the user that is stored in the elastic elements of the VSA, clutchable devices began to be investigated.

In 2013, Elliot J. Rouse *et al*. [32] investigated a device that was an advancement to the already existing field of SEA (serial elastic actuator) devices, dubbed a CSEA (clutchable-SEA). This device allowed for active movement of series springs to provide movement/stiffness to an end effector, and also for a clutch to be engaged and allow the spring to release any stored energy. This theory was mathematically proven to be sound in this paper – it was able to model human gait and reduce energy expenditure. In 2014, this same research team was able to incorporate this design into a physical prototype [3]. This prototype was tested and verified that this device was able to recreate human gait and could reduce the total energy expenditure from walking. This proves that the implementation of springs into the system of an active knee prosthesis is able to reduce energy expenditure, and, if tuned correctly, possibly even provide net-positive work at the knee joint. The AAAKP and subsequent CSEA devices developed at MIT under the supervision of Hugh Herr have had a beneficial effect on the body of research surrounding the integration of variable stiffness actuation into prostheses. It seems as though prosthetics manufacturers have not taken up the idea of this integration, and that Herr *et al.*'s work may be more influential on the academic side of prosthetic design. This author cannot trace the AAAKP or CSEA after 2013, but it seems the research team of Herr *et al*. have transitioned into

neural interface technology using the foundations of agonist-antagonist muscle groups [33].

In the time since 2014, the field of variable stiffness actuation for biomedical purposes diversified into many unique designs. These designs seek to maximize the amount of energy returned to the system via a spring mechanism, but often are too complex to be feasible. From this literature review, it seems like research in antagonistic VSA controlled prostheses comes to an end in terms of breakthrough designs around 2014. It does seem, however, that the complex mechanisms and designs that have continued, are beginning to "turn a corner" back into feasible designs, as shown in 2018 and 2021 papers [25], [34]. These papers both share an interest in using an Archimedean spiral in their design to reduce the physical space needed to control the joint. In this way, the current design is relevant. The use of a spiral spring to minimize the space needed for the device, the energy efficiency, and potential to provide net positive power at the joint are all potential benefits of the proposed design.

The concept of using a four-bar mechanism in accordance with other standard prosthesis components is not a novel concepts, indeed it is one of the core concepts of one of the most commonly known adjustable compliance knee mechanisms - the MACCEPA knee [35] utilizes a four-bar to control compliance in its first iteration (a crank-slider mechanism used to adjust the length of a spring that attached the tibial component to the femoral component – a design that was replaced with a similarly acting cam in its second iteration. A design with a similar motivation to this project in terms of a lightweight powered prosthesis that

incorporates the use of passive mechanical energy storage is the Utah knee [36], [37]. While this is a fascinating advancement, it seems as though this prosthesis only has active control over extension. While this control is vital to gait, it does not cover the entirety of the knee's functions. The symmetric nature of the proposed design would address this and be able to provide positive torque in both extension and flexion.

3. Methods and materials

3.1 Prototype building

Coming from the summer work described in Section 2.5, it was known that the four-bar mechanism would prescribe the correct path for the tibial component of the knee mechanism. It was also known that the cam-pulley-cable complex was a valid way to drive the tibia about the femur. Both facts were established by using the direct-drive gearing, also explained in Section 2.5.2. This was a simple way to drive the pulley wheels directly with no compliance introduced into the mechanism.

However, it became evident that keeping proper tension on the cables may be a challenge in a direct-drive mechanism. The idea was proposed that perhaps springs could be integrated with the cables for maintaining tension, which led to the idea of employing agonist-antagonist spring elements, as others had proposed [2], [16], [17]. Instead of straight springs and linear actuators, a novel opportunity presented itself whereby the direct-drive mechanism of our device could be entirely replaced by opposing spiral springs connected to small axial flux motors; hence the genesis of the biologically inspired knee VSA.

The scope of this thesis was not to address the motorized VSA. It is necessary to ensure that the fundamentals of this project are feasible prior to investing resources into the design of an intensive VSA. The feasibility of the mechanisms (a uniaxial "hinge" joint and a polycentric "crossed four-bar" joint) will be analyzed based on construction, physical

testing, and correlation to theory. This work also offered an opportunity to explore the influence of the kinematic constraints of the artificial knee on how a fully motorized VSA may behave dynamically, which could offer new insights into the biological function of the cruciate-bone complex in animal knee joints.

3.1.1 Experimental goals

The direct-drive system of the large, summer work model needed to be replaced with a spring-driven mechanism that could provide a variable amount of torque on the pulley driving shaft based on inputs to the spring (Section 1.3). This would be done by treating the spring system and the cam-pulley-cable system as independent. The mating of these two systems simply required the connection of the output shaft of the spring device to be attached to the input shaft of either pulley. Therefore, design optimization was performed on both systems simultaneously.

The overarching goal of this prototyping was to achieve a mechanism that has independent control of both the stiffness and position of the tibial component. The control of stiffness and position would allow the physical prototype to be compared against a simulated version of the knee mechanism. Indeed, this simulated mechanism and its comparisons to the physical mechanism acts as a substantial contribution to this work. A description of the creation and optimization of this simulation is not discussed in this work as it was done prior to this work, and the physical model stems from some of the basic geometries

introduced in this simulation. A description of how the simulation works is given in Section 4.1.

3.1.2 Design

Spring Mechanism

As this design was split into the creation of the spring mechanism and the cam-pulley-cable mechanism, a description of the spring system will be presented. As the design of a custom spiral spring that would fit inside each pulley was beyond the scope of this project, an analog would need to be created that would give equal control over the tension of the spring and position of the output rod. This analog consisted of a double torsion spring connected advantageously on either side to allow for adjustment of its "free" end. This spring system can be seen in Section 3.2. The design went through multiple iterations to be able to find a method of isolating the torsion of the spring from the movement of the rod. One method saw the "legged" end of the double torsion spring bend back into the output rod to establish a rigid connection between the fixed "legged" end of the spring and the pulleys, but this was deemed un-usable due to the stress concentrations that would be placed on the spring. The method that was selected was to affix the "legged" end of the spring to a c-shaped aluminum piece that would be also fixed to the output rod. This meant that any movement of the pulley would be linked to the movement of one end of the double torsion spring. The other end of the torsion spring would also rotate about the output rod but would be connected to it via the spring. The spring was connected on the "free" end by a second, smaller c-shaped aluminum piece that would sit inside the output piece. In this way, the

"free" end of the spring could be adjusted to create torsion on the output shaft. To provide a constant torque on the output shaft, the "free" end would need to be held at a given displacement angle relative to the "fixed" end. Therefore, the entire spring system was placed inside a circular angle gauge with slots that allowed the free end to be adjusted and held relative to the fixed end.

Cam-pulley-cable system

Second, analysis of the cam-pulley-cable system. It had been established from prior work that the wrapping of the cables around the pulleys, onto a cam surface, and terminating on the tibial component was a valid way to actuate the tibia about the femur. The dimensions of the large model (Figure 8, Figure 9) were simply a scaled version of the dimensions that were to be used in this work. Therefore, all of the relative positioning of pulley centers and cam centers was already done. Smaller versions of the model in Figure 8, Figure 9 were printed using PLA and simple iterative design was performed to find the proper lengths of the tibial components, infill percentage, and proper mounting points on the prints, *etc*. One key component was ensuring that the pulleys, and pulley shafts, were secured and in a position where they could be accessed by the spring device's output shaft. An explanation of this positioning can be seen later in this section.

The knee prototype went through multiple iterations before being viable for testing. Full images of previous versions are shown in Appendix B.

3.2 Prototype iterations

The idea behind the first prototype design after the large, orange, direct drive prototype was to be able to have freedom to move the drivetrain above the knee mechanism, where a femoral socket attachment may be (Figure 11). Therefore, the drive mechanisms were to be linked to the pulleys through bevel gears, as the pulley shafts run laterally across the knee joint, and the drive shafts would run vertically to them. In an effort to reduce the size of the prototype, and because power is transmitted through the bevel gears regardless of where the drive gear is meshed to the pulley gear, the drive mechanisms were placed below the tibial component. In theory, the idea to have a set of meshing gears between the input angles of the spring device gives further freedoms to the user, changing gear ratios to provide differing input/output ratios from the spring device to the pulley wheels. Unfortunately, the bevel gears proved to be unreliable given the nature of the prototyping apparatus. Without the proper constraints or supports on the gears, stemming from the size limitations of the prototype, the gears would come out of mesh and bind, preventing the pulley wheel from turning in a predictable fashion with the input shaft. A significant amount of stresses are placed upon the teeth of a bevel gear while in motion, and it is crucial to the smooth interaction of gears that they be constrained in all directions [38]. This problem was multiplied when substantial pretensions were placed on the drive shafts, causing unwanted movements of the shaft off-axis. Therefore, the bevel gears were eliminated and the directions of the shafts changed.

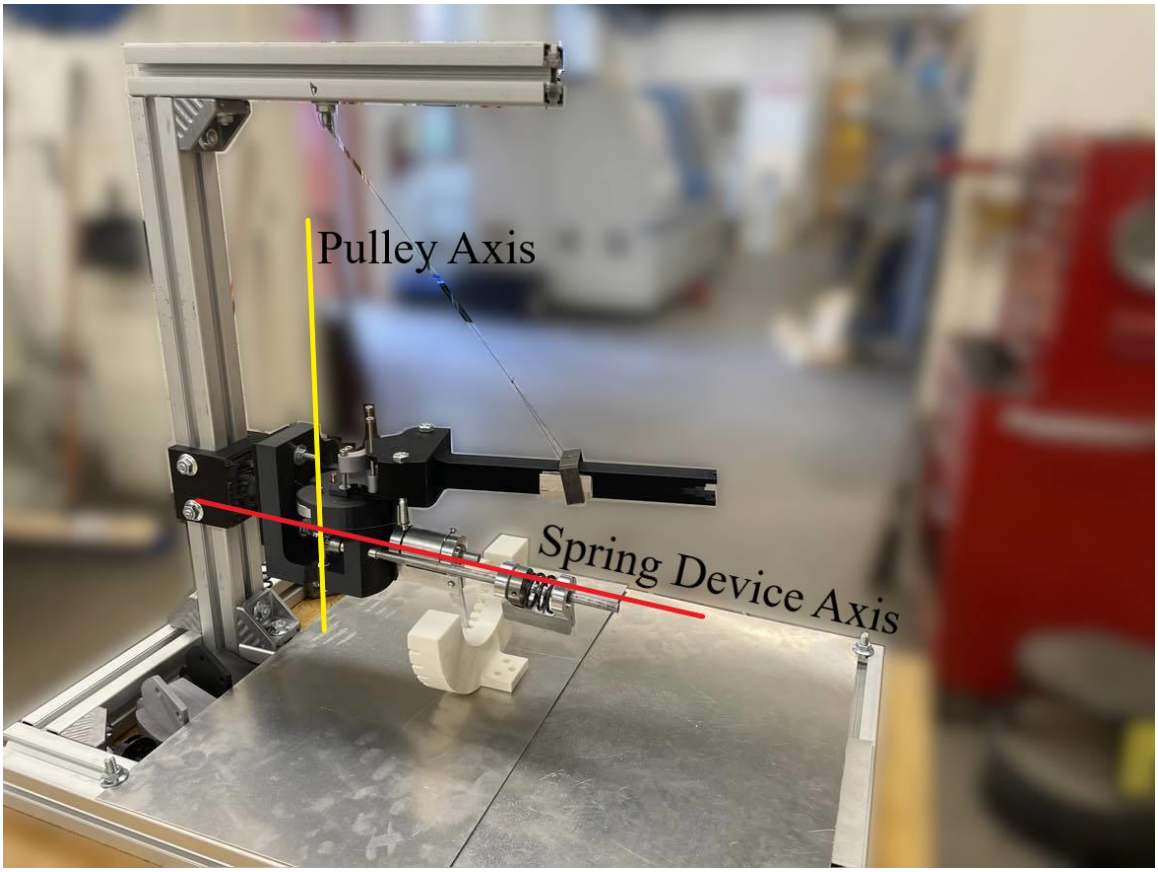

Figure 11: Initial design for physical prototype.

One benefit of the bevel gears was the ability of the drive system to be compact in the axial direction – that is, the direction parallel to the pulley shafts (see Figure 11). If no gearing could be used to transfer power to the pulley shafts, the spring mechanisms would need to be colinear with the pulleys. Meaning, the mechanism would need to be raised higher to allow for space below for the springs. This led to the second iteration of the device, where both spring devices were placed directly below the pulley wheels. This placement eliminated the bending moments on the input shafts but introduced the issue of practically implementing collinearity between the pulley shaft and the spring device shafts. Brace collars were designed to ensure the (now very long) shafts did not drift away from

linearity. Ball bearings on these collars also enabled smooth, low-friction rotation. Another benefit of this setup was that it was more similar to how the device will be in the future. Instead of the spring being located inside the pulley, it is a simple expansion to say the springs are located just outside the pulley. This setup was used for multiple rounds of data collection before an issue with the data collection became evident. As the pulleys are located so close to each other, and the space for the angle gauges/spring mechanisms is so large, the spring mechanisms had to be located on different planes so they would not interfere with each other's movement. This can be seen in Figure 12.

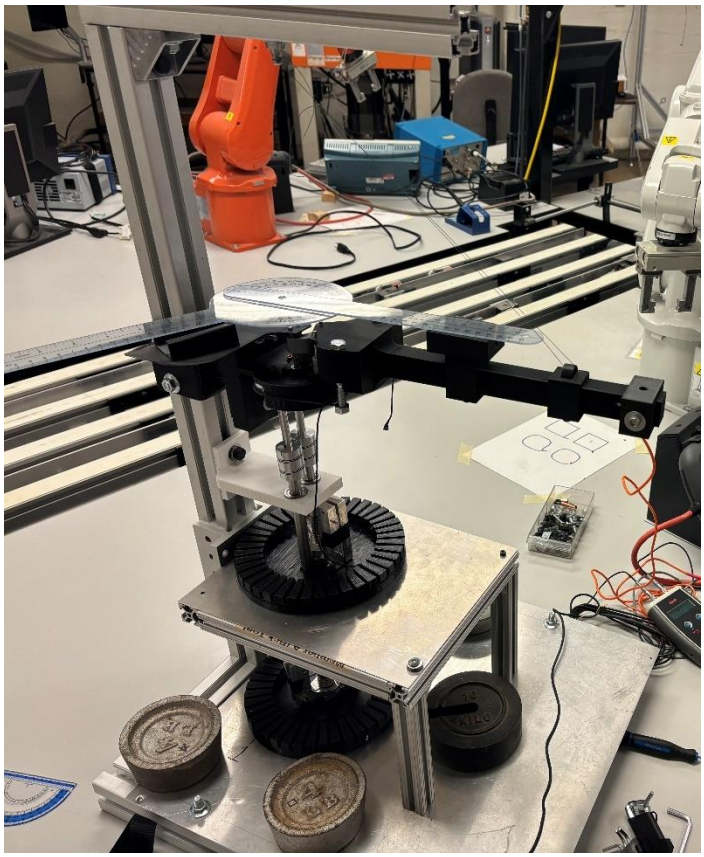

Figure 12: Second iteration of physical prototype.

To reach the bottom spring mechanism, the top angle gauge needed space to allow a shaft to pass through it. Therefore, the top spring mechanism was not able to complete a full rotation and a range of stiffness possibilities could not be explored. This data would be required for a full and complete dataset, so more possibilities needed to be created. This led to the third and final iteration of the mechanism.

The final mechanism structure placed one spring mechanism on top of the knee mechanism and one below. This allows for each pulley to have a colinear rod extend to a spring mechanism/angle gauge that can freely turn 360 degrees. It also introduces more issues with the ability of the rods to remain in-line with the pulleys. As one spring mechanism is now completely above the knee, considerations had to be made. First, the shaft needed to be vertical so unwanted off-axis rotations seen by the pulley would be negligible. This was dealt with by having supports attached to the vertical extruded aluminum that ran behind the prototype that had a vacancy for a ball bearing situated directly over the pulley shaft. Next, the weight of the spring mechanism and shaft would have to be held in some way so the pulley would not fall or have any vertical forces (apart from gravity) acting on it. This was done via a collar placed on the drive shaft as it passed through the angle gauge. This collar, placed on the inner ring of a ball bearing which the shaft also passed through, transferred the weight of the shaft and spring mechanism to the upper plane which was supported by the vertical extruded aluminum. The final mechanism has been broken into the top, middle, and bottom sections, as well as shown in its entirety, in Figure 13 to Figure 18.

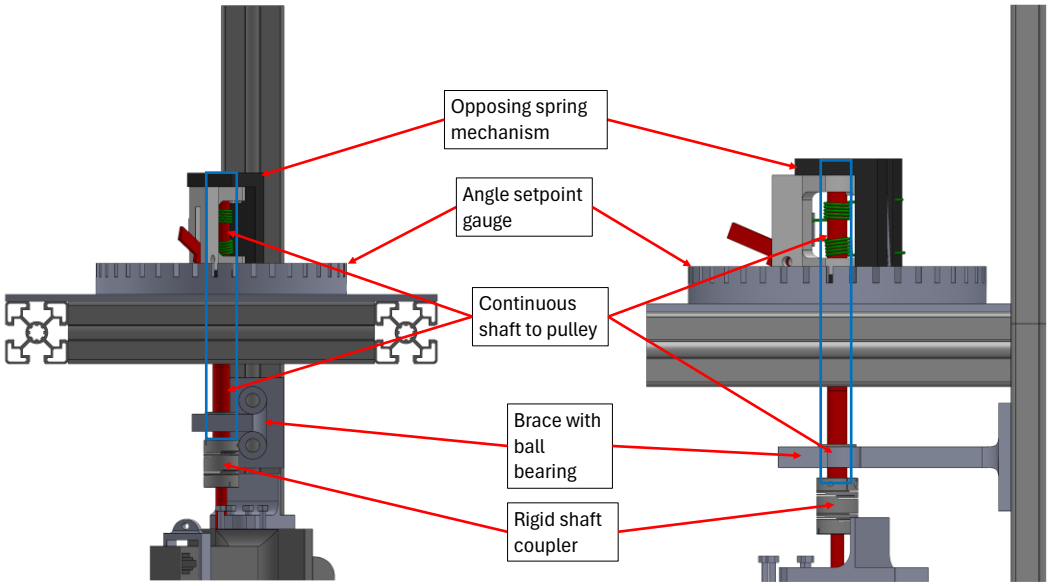

Figure 13: Physical prototype, CAD model, upper detail

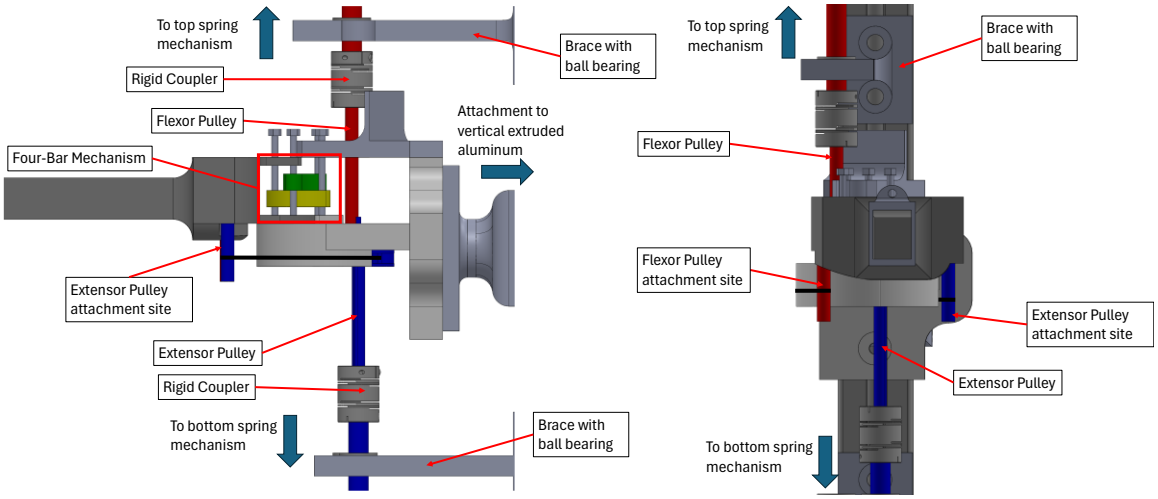

Figure 14:Physical prototype, CAD model, middle detail

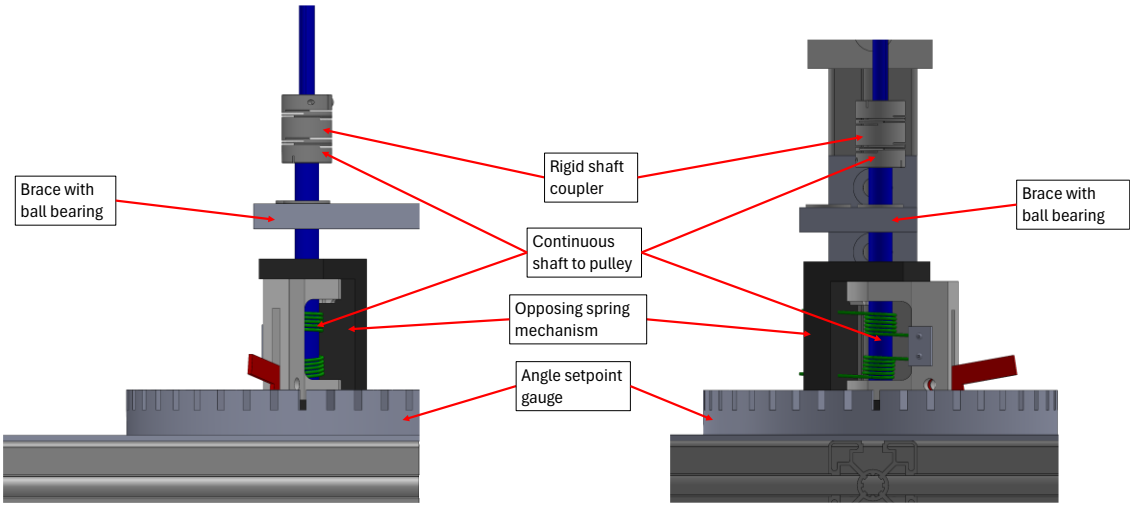

Figure 15: Physical prototype, CAD model, lower detail

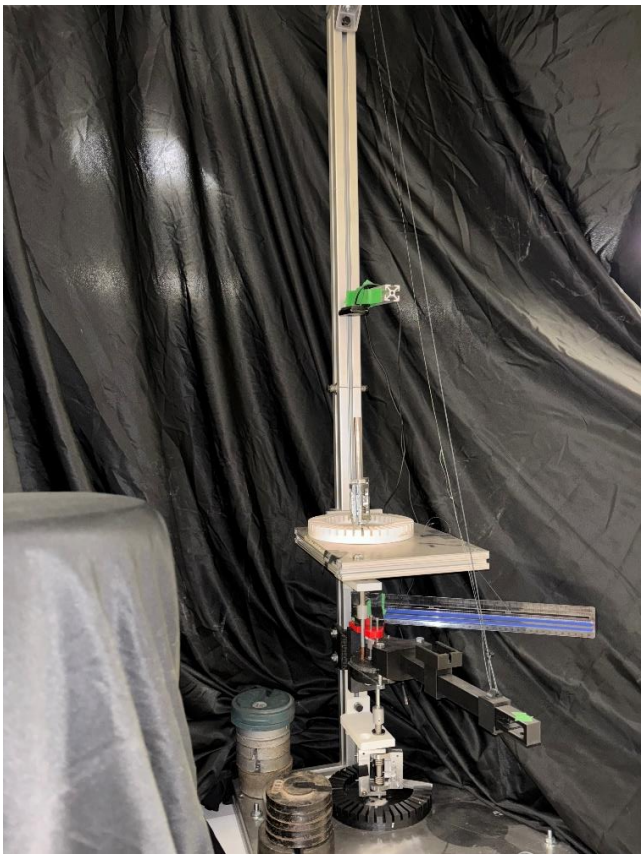

Figure 16: Physical prototype

Figure 17: Physical prototype, middle - lower detail

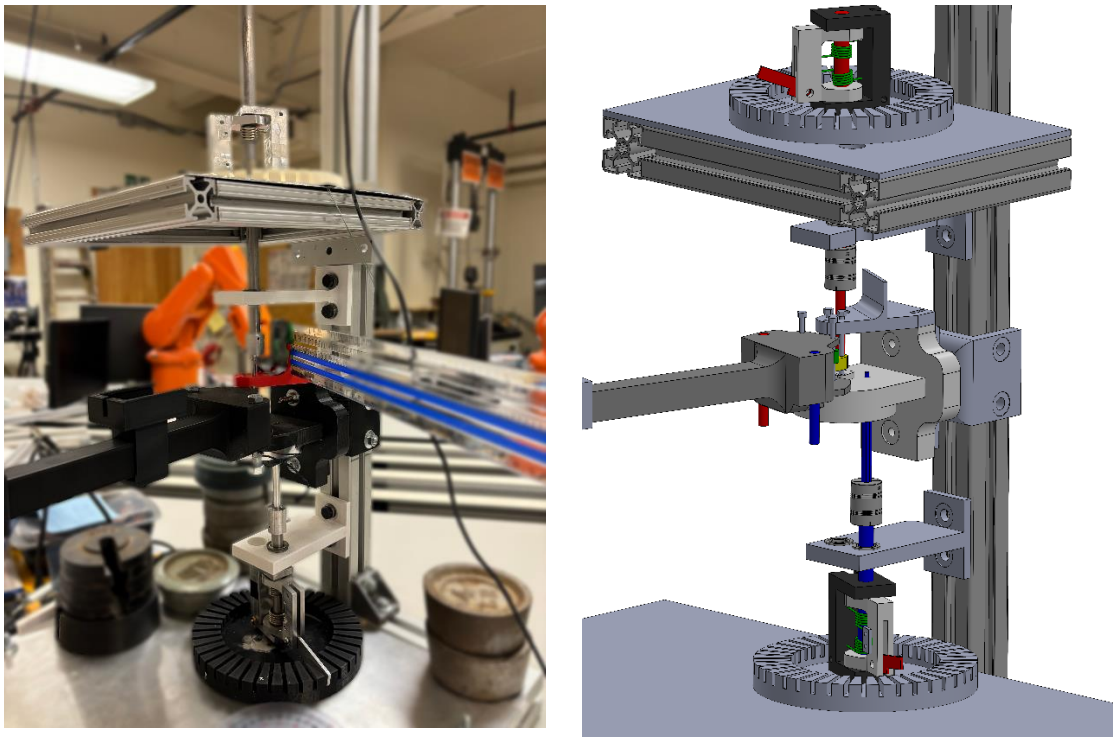

Figure 18: Final testing mechanism (left) and detail of femoral-tibial interface

3.3 Opposing spring mechanism

The spring mechanism is used to adjust both the stiffness and position of the knee. Adjustment of the position is performed by moving both spring mechanisms in the same direction. Adjustment of the stiffness is performed by adjusting the load on the spring via the spring setpoint adjustment piece in opposite directions on either spring mechanism. As the "free" end of the torsion spring is rigidly attached to the rod via the displacement output component, any angular displacement of the spring setpoint adjustment piece will cause a torque, relative to the spring stiffness, to be placed on the pulley. The farther the spring is displaced, the higher the static torsion on the pulley and the higher the tension on the cables connecting to the tibial component. These parts can be seen in Figure 19.

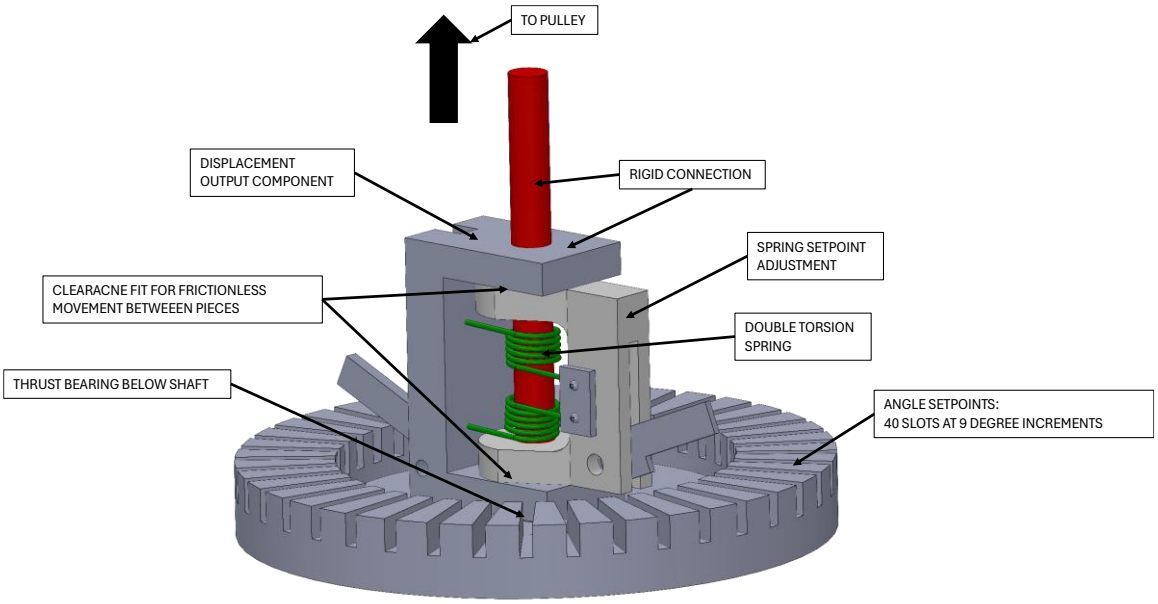

Figure 19: Overview of spring mechanism.

Active region

There exists a region of the mechanism wherein there is very little resistance during the movement of the tibia. This region has come to be known to the author as the mechanism's "Active region". This region is an artifact of the interplay between both the spring mechanisms, the pulleys, and tibial displacement.

Initially, the spring mechanisms start with no displacement of the springs – their resting position. Any movement of the tibia will pull on, and relieve tension on, the corresponding cable (flexion of the knee will cause the extensor pulley to unwrap, as it is being pulled away from it, and cause the flexor pulley to wrap – *if it is able to do so*). Movement of a pulley will cause the displacement output component to either tension or un-tension the torsion spring, as they are rigidly connected. When both spring mechanisms are at their neutral position, it can be understood that tibial movement will only flex one of the springs, as one pulley will be moved via the cables, and the other pulley will not move as the cable cannot force the pulley to spin and take up the slack.

Now, consider another scenario where both springs are pre-tensioned to an angle of 36 degrees. Movement of the tibia will again cause one pulley to release more cable and tension it's spring, but now because there is a pre-tension on the opposite pulley, it will have the ability to take up the slack being given to it. That is, until the tibia has displaced so far that the receiving pulley has completely un-tensioned the torsional spring. At this point, the cable will slack, as the spring will not continue to rotate through its neutral

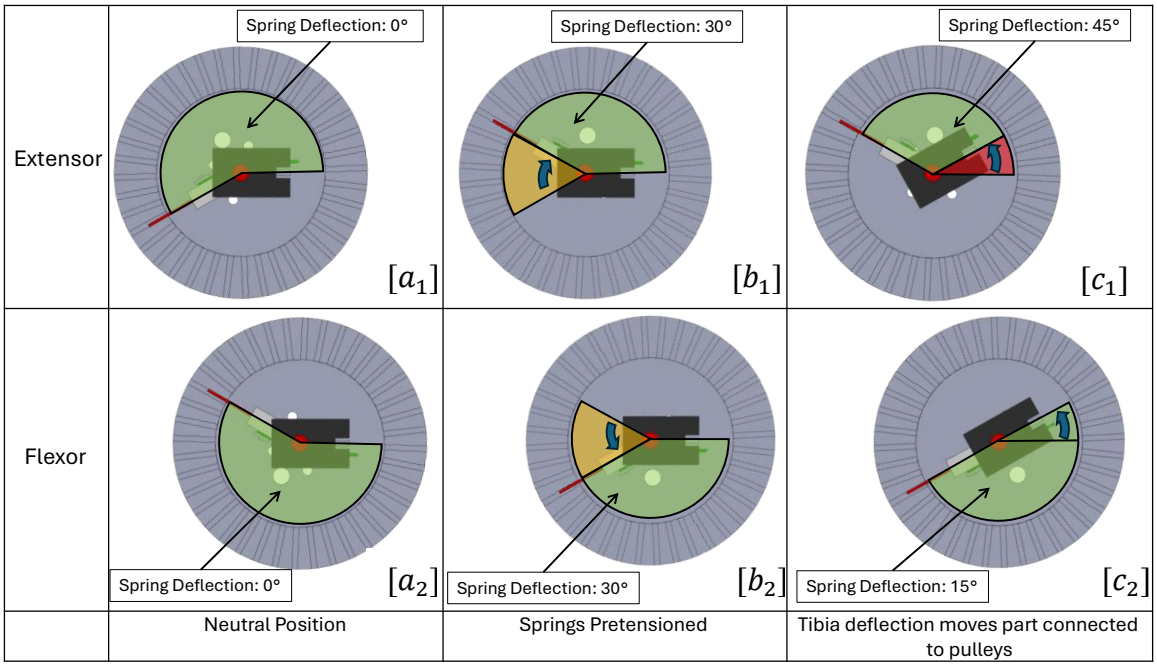

Figure 20: Top-down view of spring mechanisms when displacing tibia

position to keep tension on the cable. This pre-tensioning and subsequent tibial movement, which influences both springs, can be seen step-by-step in Figure 20.

This region, accounting for both flexion and extension, is the active region. In this region, after energy has been expended to deflect the springs in some amount of pretension, the springs are "trading" energy stored between them in a 1:1 fashion. It can be imagined that the smaller the angle of twist of the spring, the smaller the active region, as the springs have no ability to give/take tension from the cables. Likewise, the larger angle of twist of the spring, the larger the active zone, as both springs apply a pre-tension to their pulleys, and slack is able to be taken up by the receiving pulley. In this region, the tibia shows very little resistance to being displaced (small stiffness) but is able to be put into place and

remain there due to the trade-off nature of the pulley cables (high position controllability). The capacities and repercussions of the active region is investigated in Section 5.

3.4 Experimental protocol

3.4.1 Sensors

The primary variables of interest for this project are the displacement angle of the tibia relative to the femur, and the resultant stiffness of the tibia given an input torque from a load applied perpendicular to the tibia of the prototype device.

First, the position (angle) of the tibia needs to be measured. As measuring position in space with a device such as an IMU is troublesome, and we only require the relative angle of the tibial component to the fixed femur, a measurement device that can accurately tell the angle between two fixed positions is needed. A goniometer is a simplistic device used in orthopedic medicine to measure the angle between body segments. A common use for a goniometer is to measure the angle between the femur and tibia, also known as the knee angle. Typically, a goniometer is made of two pieces of plastic joined together at a fixed center with a 360-degree protractor at the joint which is used to measure the angle between both ends of the instrument. An example is shown in Figure 21.

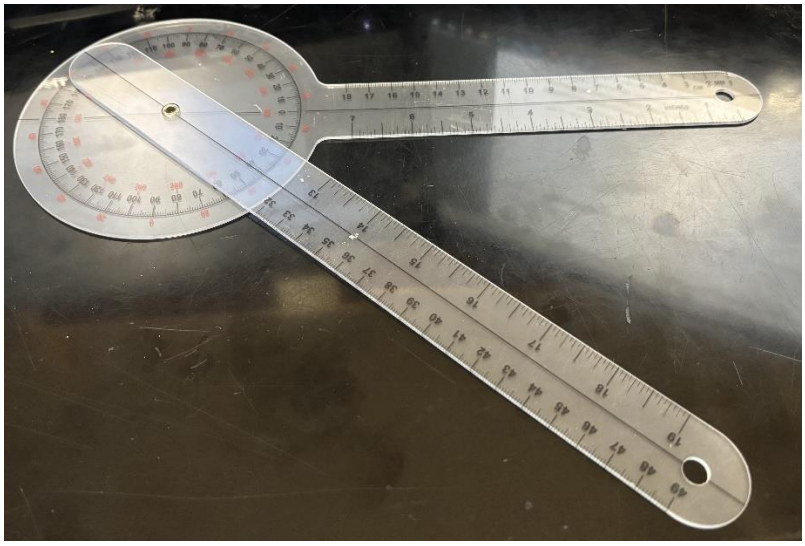

Figure 21: Goniometer used in testing

The main use of this angle gauge is to verify the knee angle set by the spring mechanisms. If a test is to occur at a knee angle of 30 degrees (see Section 3.4.2), the goniometer is used to ensure that the initial position of the test is at 30 degrees. This can be seen in Figure 23. The stiffness of the mechanism is calculated using the amount of force required to displace the end of the mechanism a set number of degrees while the spring mechanisms are at a set deflection. It has been hypothesized that the higher the deflection of the torsional spring, the more force it will require to displace the end of the tibial component. To determine the amount of force required to displace the end of the tibia, a measurement device would need to excel in one-sided tension testing. A calibrated scale would be able to provide the necessary data. Taking both resolution and cost into consideration, a simple luggage scale was determined to be able to produce quality data without the need for specialty fixation methods or DAQ boards. An image of the luggage scale is provided in Figure 22.

Figure 22: Luggage scale used for tension testing

The luggage scale used was tested and could repeatably give repeat mass weights to 10-gram accuracy. These tests verified that this scale would be reliable for testing.

As this scale will be pulling the tibial component about its axis of rotation, it is important to keep the strap of the scale as close to 90 degrees to the tibia to ensure all force it takes to move the tibia is felt by the scale.

Motion during testing was recorded via a three-camera setup coordinated through the video capture software OBS Studio. The camera setup was used to coordinate viewing of two angular variables and the force variable during testing. The OBS camera setup is centered around the main, top-down video feed of the entire mechanism, and two other specific views are superimposed onto this feed. All cameras and videos live update in the same window, allowing for instantaneous capture of three video feeds on one screen.

The view from the top camera is shown in Figure 23 and was used to determine the location of the tibia. The entire mechanism was placed and centered on a large-scale protractor to

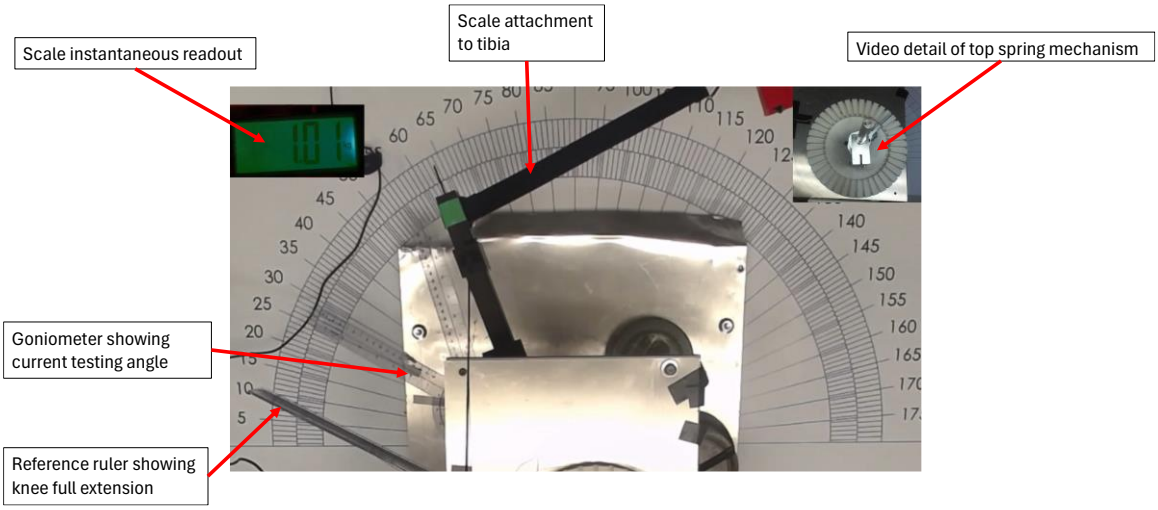

Figure 23: OBS camera setup to capture all relevant data

be able to have a rough idea of the tibial location at all times. For more precise angle measurements, either the goniometer or digital methods were used directly from the recorded images, which is explained later. From this camera view, one can see the location of the tibia, the entire protractor, a placed goniometer at a specific testing angle, and the reference ruler that shows where full extension is for this mechanism.

The second camera was mounted slightly closer to the mechanism, just above the flexor setpoint adjustment control. This allowed for the identification of when the spring mechanism was reaching the end of its usable twisting angle, and to see how far the spring has deflected. As these are linear springs, a simple analysis of how far the spring has deflected will yield its supposed output via Hooke's law. This spring reaction force analysis is further investigated in Section 4.3.

Figure 24: Camera mount for the luggage scale.

The final camera was pointed directly at the readout screen of the luggage scale. This allowed for more accuracy in data processing, as during analysis every change in the scale could be noted. The camera was mounted to a specially designed 3D printed part that could be placed on the luggage scale and hold the camera at a proper distance for a clear picture. This is shown in Figure 24.

For analysis, the recording shown in Figure 23 was brought into a kinematic analysis software called Kinovea. This software, typically used in biomechanical analysis, was helpful in this context as it allowed for frame-by-frame scrubbing and angle viewing. Therefore, every time the force sensor changed its readout, the angle of tibial deflection could be recorded. A screenshot of this analysis is shown in Figure 25. It can be seen that at any frame where the video is stopped, the built-in goniometer tool can give the angle of the tibia from horizontal (right hand shaded region), as well as the force sensor readout. This angle can be compared to the offset of the knee's fully extended position from

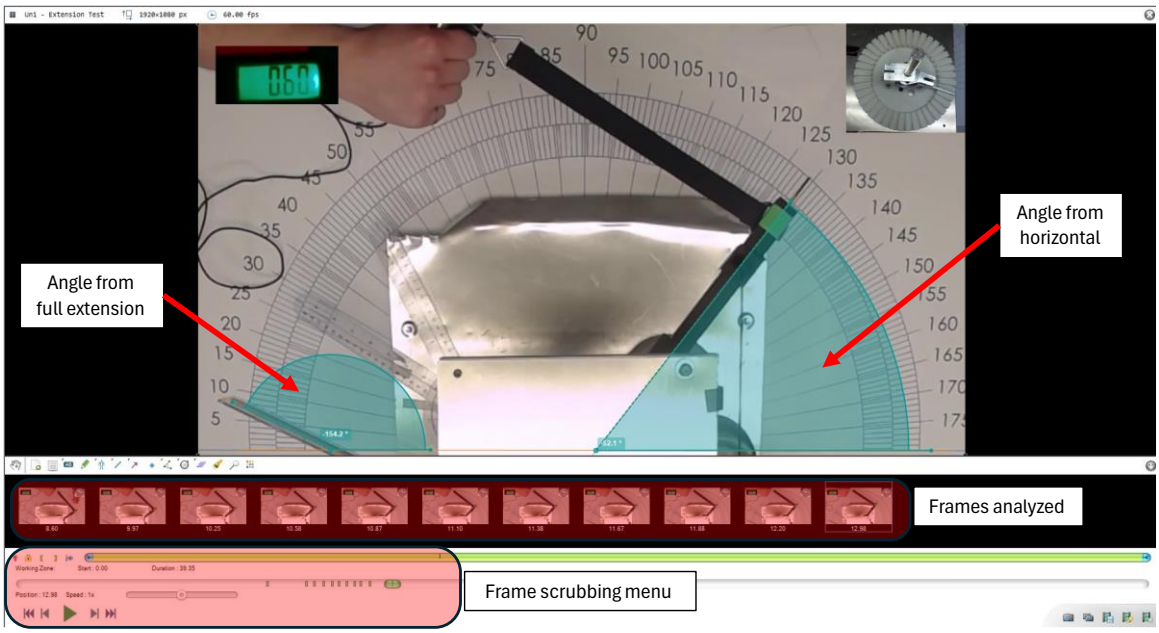

Figure 25: Screenshot of Kinovea analysis screen

horizontal (left hand shaded region). In this way, the angle from horizontal can be translated into knee flexion/extension angle. This was done for the entirety of the recorded test, at increments of approximately 15 frames.

3.4.2 Active zone testing

An important aspect of the mechanism was the ability of the knee to have stiffening characteristics within its active zone. As mentioned in Section 3.3, this is the region where both the extensor and flexor springs are providing opposing torques on the tibia through their cable attachments. It seemed at first that there would be no stiffening activity in this region, as the tibia was relatively easy to move throughout it and would stay in pace once force was no longer being placed on the end to move it. However, this region is important to the use of the device and to having a large range of stiffening capabilities. And theoretically, if two opposing torques are fixing an object in place, the object should be

harder to displace the larger the opposing torques are. Thus, a test of the stiffening capabilities in the active zone is required.

First, the active zone of the mechanism would need to be identified. This was done physically, by displacing the tibia until a point where it would "spring back" when released. The angle where the tibia would come to rest was considered to be one end of the active zone. This was repeated on the opposite side to find the range of the active zone. It follows from the explanation of the active zone that the more pretension the opposing springs are under, the larger the active zone will be.

Once the active zone was established, the tibia was placed at the extension limit of the active zone, to be pulled into flexion. The luggage scale was attached to the end of the tibia via a void in its side, and the tibia was pulled through the active zone. The purpose of this test was to determine if a larger spring pretension would cause the tibia to stiffen and be harder to displace inside the active region. Therefore, this test was performed at both 36 and 54 degrees of spring pretension. A baseline of 0 could not be established, as with no pretension on the springs there would be no active zone, and any displacement of the tibia would immediately cause one of the cables to slacken. The results of these active zone tests are shown in Section 4.

The dis-inclusion of motors limited the tests that could be performed. The active zone created by the pretension on the spring devices is limited by the set amount of spring deflection added. This means that when one spring is unloaded, the cable will fall from the

pulley and the test would need to end. To be able to test stiffness control and modulation in the full range of human gait, a dynamic control scheme would need to be implemented to ensure tension is kept on the springs, ensuring the knee is always being acted on by forces in both the extension and flexion directions. In the current setup, the testing done is evaluating the spring mechanisms' ability to resist external torques at differing amounts of pretension.

3.4.3 Single-sided testing

Both the extensor and flexor spring mechanisms have been established to work in conjunction to control the position and stiffness of the mechanism. To fully characterize how the mechanism works and to understand the contributions of both springs, it was determined that both springs would need to be tested independently. This testing would mainly serve to verify the simulation models, as it was hypothesized that the changing moment arm from the COR of the mechanism to the cable attachment would give a mechanical advantage to the knee in high flexion/extension scenarios.

As this single sided test needed to be performed in both flexion and extension, the most needed to be made from the available range of motion that the spring mechanisms would allow. Therefore, the flexion tests (pulling into extension and observing the resistance of the flexion spring) would need to start at a high level of flexion and pull as far as they could. Likewise, the extension tests (pulling into flexion and observing the resistance of the extension spring) would need to begin at full extension and pull as far into flexion as the spring mechanism would allow. The spring mechanisms were somewhat limited in their

testable ranges, as spring deflections past approximately 90 degrees would cause the setpoint adjustment piece to run into the displacement output component.

This testing would be helpful in verifying that the model yields similar results to the simulation. In the simulation, the torque provided by each spring mechanism (extension and flexion) is calculated and used to find the overall stiffness of the joint. A more detailed explanation is given in Section 4. If the results of this physical test align with the simulated results, then more trust can be placed on the simulated results

4. Results

4.1 Simulation

All quasi-static testing done in the results that follow are compared to a simulated version of the testing done in Matlab. These comparisons help to verify that that the simulation is yielding results that can be relied upon in lieu of further testing. If displacing the distal portion of the tibia and using its resistance to movement is working backwards to find knee joint stiffness, then the simulation results are working forward. The simulation uses the spring constants, spring (pulley) displacements, radii of pulley wheels and cam surfaces, and cable forces to determine the stiffness of the joint. A description of how the simulation finds stiffness is derived. All relevant variables for the simulation are defined in Figure 26.

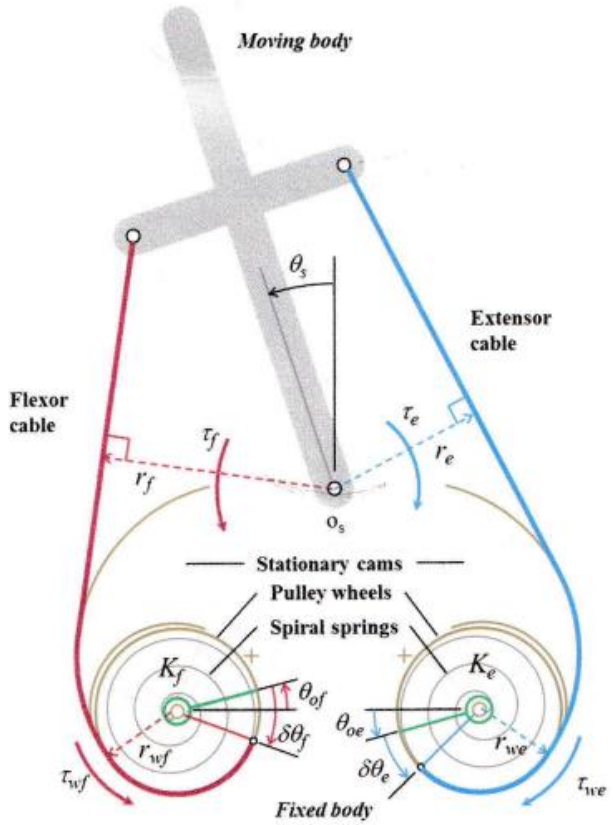

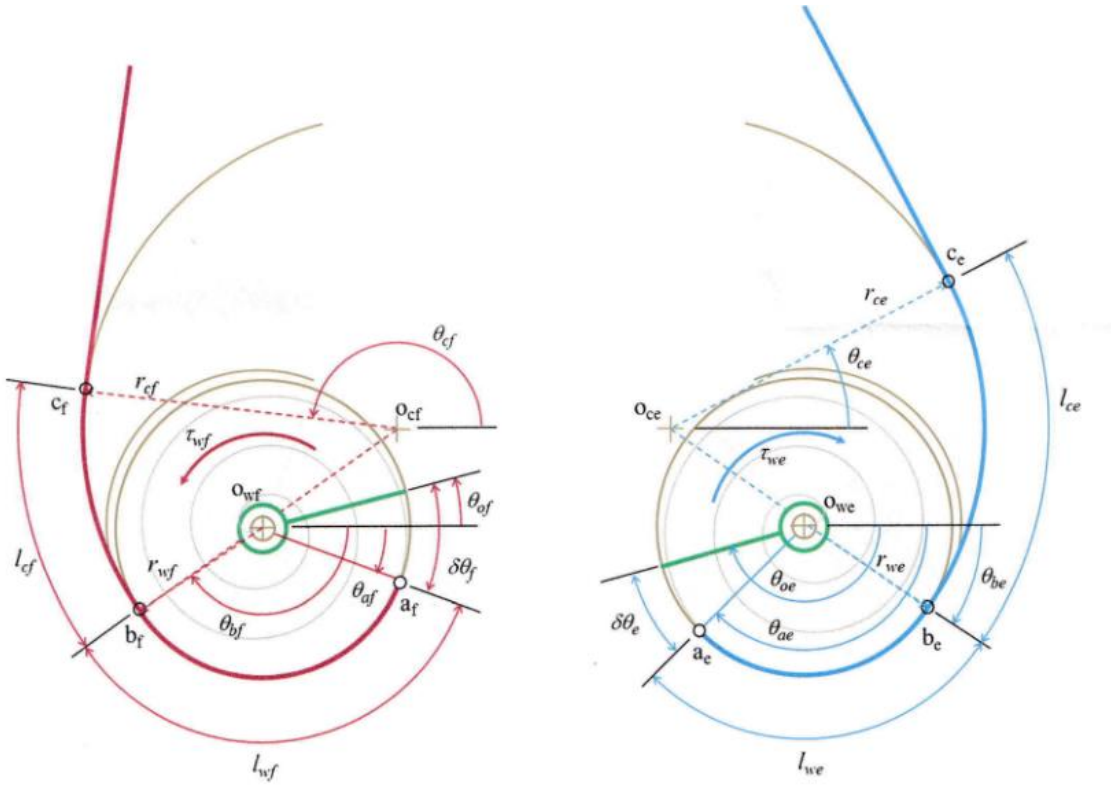

Figure 26: Explanation of variables used in calculations. Explanation from ICR above (a). Detail of variables used to define spring motion below (b)

It can be seen that the two torques seeking to move the tibia in either the extension or flexion directions are represented as τ_e and τ_f respectively. In order for the tibia to not be extending or flexing (remain in a constant position), the following equality must be true at any static position:

$$\boldsymbol{\tau_e + \tau_f = 0} \quad \textbf{(4.1)}$$

In terms of variables that can be controlled, the extension and flexion torque are simply the amount of force in the cables and the radius between the joint COR and the cable. Therefore,$\boldsymbol{\tau_e + \tau_f = 0}$ equation (4.1) can be rewritten:

$$\boldsymbol{r_e F_e + r_f F_f = 0}$$

(4.2)

where r_e and r_f are known distances. As cable forces will be unreliable as a measured value, and there are ways to determine these forces, the following substitutions can be made to eliminate the dependence on cable force as a value:

$$r_e \frac{\tau_{we}}{r_{we}} + r_f \frac{\tau_{wf}}{r_{wf}} = 0$$

(4.3)

In equation (4.3), τ_{we}, τ_{wf} and r_{we}, r_{wf} are the torques on the respective extensor and flexor pulley wheels, and the radii of the respective extensor and flexor pulleys. Due to the nature of the system, and the fact that the deflection of the spring directly inputs a torque to the pulley, τ_{we}/τ_{wf} can be replaced with spring deflections and the spring constants, in accordance with Hooke's Law, to yield the following:

$$r_e \frac{K_e \delta\theta_e}{r_{we}} + r_f \frac{K_f \delta\theta_f}{r_{wf}} = 0$$

(4.4)

Equation (4.4) gives the user the ability to find the flexion and extension torques at any amount of spring deflection, which can be set by the user. An important ratio that can be pulled from equations (4.3) and (4.4) is the ratio of the cable moment arm to the pulley radius, which can be defined as:

$$U_e = \left|{}^{r_e}/_{r_{we}}\right| \qquad U_f = \left|{}^{r_f}/_{r_{wf}}\right|$$

(4.5a, 4.5b)

Using the equations that govern how much torque is provided by both the flexor and extensor springs, and therefore how stiff the knee is, an equality can be furthered to extend

to external forces placed on the tibia that would deflect the joint. This equality constraint can be seen in the following derivation:

$$\tau_e + \tau_f = 0 \text{ for static stability}$$

If we allow this to be not equal to zero, we can say the following:

$$\tau_e + \tau_f = \tau_K \quad \textbf{(4.6)}$$

where τ_K is the mechanism resistance torque. This is an important value if the knee is exposed to an external torque seeking to displace the tibia. This external torque can be called τ_G. Therefore, for static stability under an external load, the following equality must be true:

$$\tau_K + \tau_G = 0 \quad \textbf{(4.7)}$$

From equations (4.1) – (4.5a, 4.5b) above, this can be rewritten as the following equality:

$$\left(K_e U_e \delta\theta_e + K_f U_f \delta\theta_f\right) + \tau_G = 0 \quad \textbf{(4.8)}$$

Therefore, in all tests requiring a simulation to determine a required external torque to compare against a physical test where external torque is being recorded, equation (4.8) can be rearranged to yield:

$$\tau_G = -\left(K_e U_e \delta\theta_e + K_f U_f \delta\theta_f\right) \quad \textbf{(4.9)}$$

It can be seen then that the simulation will provide data that comes from completely interior variables and yields external values. Using comparisons between this simulation and

completely external values provides a robust way to determine the effectiveness of both the simulation and physical testing.

4.2 Active zone testing

4.2.1 Polycentric

The majority of the tasks required by the knee joint will be done when both agonist and antagonist springs have a tension or preload on them to give the leg a desired stiffness/position. To assess how the proposed knee joint can handle these tasks, the springs were preloaded and the active region that resulted from the preload was assessed. Next, the tibia was pulled through that region and the force required to do so was recorded. This was done for two spring preload values to assess if stiffness could be modified in a predictable fashion. The results are shown in Figure 27, with a comparison to the simulated data.

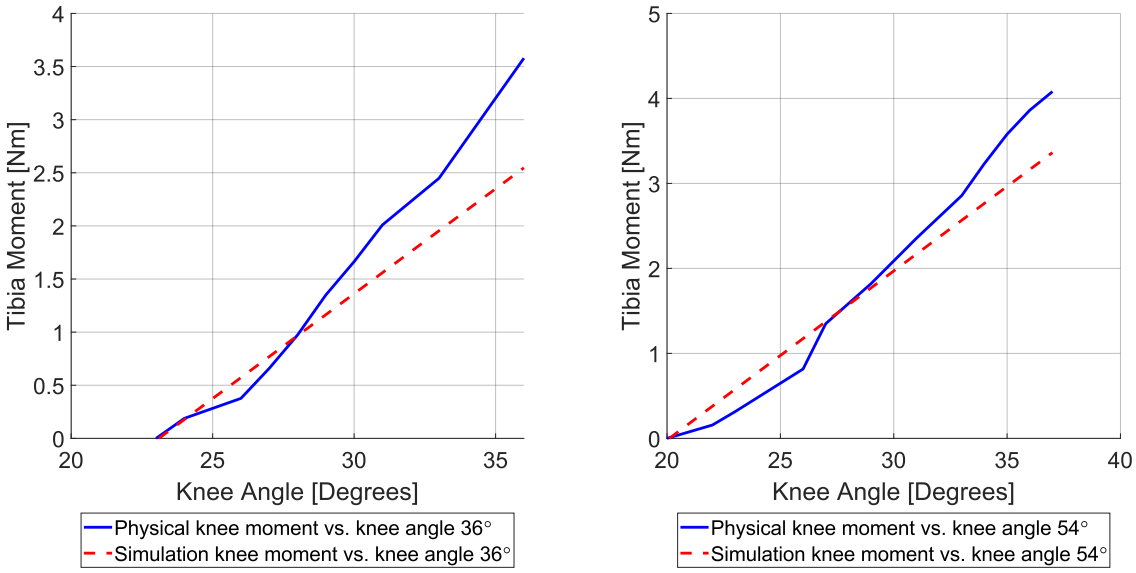

Figure 27: Active zone force requirements: 36 (left) and 54 (right) degree spring pretension, 30 degree knee angle, polycentric mechanism

The knee data was collected by recording the force required to displace the end of the tibia. This force is multiplied by the distance from the COR to the pulling location at the end of the tibia. The simulation data was found by working backwards from the displacements of the springs during deflection, as explained previously. The spring displacements generate a torque on either end of the antagonist joint, pulling the tibia. Using this joint and knowing that at any point the joint can be stopped and will not "spring" back, the equality in equation (4.7) can be verified.

To verify the validity of these tests, and to ensure that controllability of stiffness would be available with all knee flexion angles, knee angle was considered for the active zone testing. The results of the same test are shown in Figure 28 with a knee angle of 60 degrees.

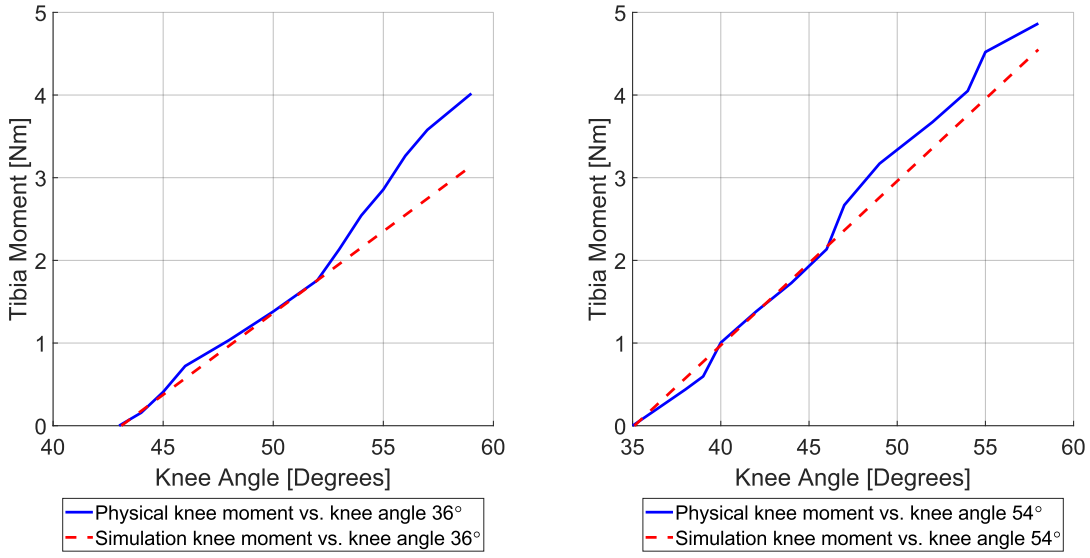

Figure 28: Active zone force requirements: 36 (left) and 54 (right) degree spring pretension, 60 degree knee angle, polycentric mechanism

The tests performed at 60 degrees were done identically as at 30 degrees and were compared against the same simulation, which was run each time with the correct corresponding initial and terminal angles and spring deflections. A comparison was also drawn between the required knee moment to displace the tibia at both 36 and 54 degrees of spring pretension to identify if stiffening behavior was exhibited while holding deflection constant. These comparisons are shown in Figure 29.

The comparisons between the pretension in the spring and moment required to displace the tibia seem to be obvious, but a further analysis of the stiffness these curves yield will need to be discussed in a further section. Tabular data of these tests can be seen in Table 1 and Table 2.

Percent differences (used in tables) presented are calculated as follows:

$$\left|\frac{Difference}{Average}\right| \times 100 = \left|\frac{a-b}{\left(\frac{a+b}{2}\right)}\right| \quad \textbf{(5.10)}$$

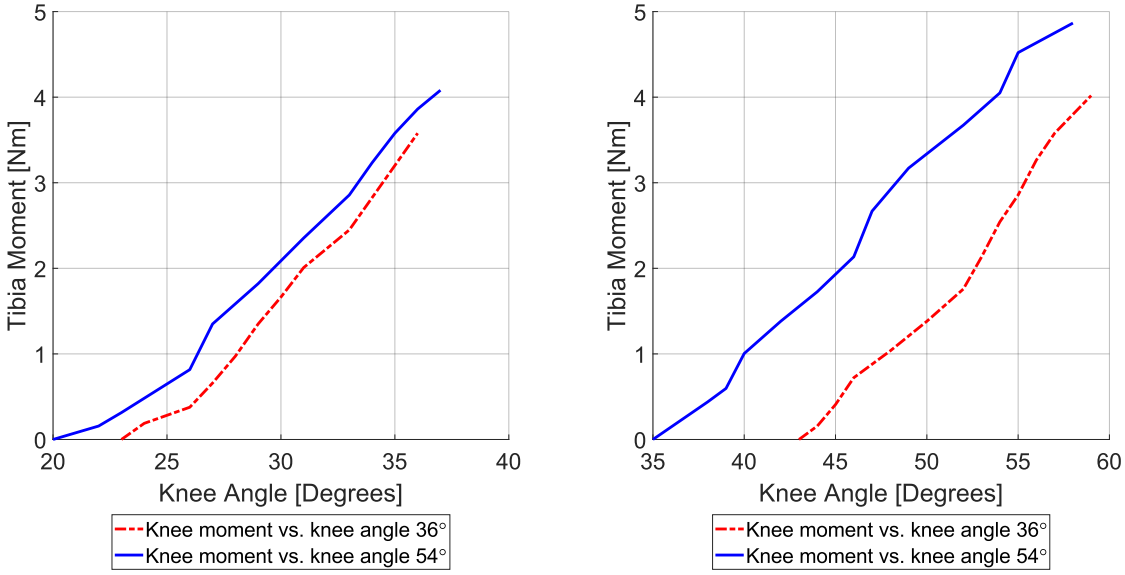

Figure 29: Comparison between pretension amounts at 30 (left) and 60 (right) degree knee angle, polycentric mechanism

	30 Degree KA		
	Peak stiffness at 36 pretension	Peak stiffness at 54 pretension	Difference (%)
Simulated	2.547	3.362	+27.594
Actual	3.579	4.081	+13.115

Table 1: Differences between peak stiffness values at 36 and 54 degrees of spring pretension. Polycentric, 30 degree knee angle.

	60 Degree KA		
	Peak stiffness at 36 pretension	Peak stiffness at 54 pretension	Difference (%)
Simulated	3.142	4.55	+36.588
Actual	4.018	4.866	+19.082

Table 2: Differences between peak stiffness values at 36 and 54 degrees of spring pretension. Polycentric, 60 degree knee angle

4.2.2 Unicentric

The test of the active zone resistance was performed with the unicentric (hinge) joint on the knee prosthesis. All testing procedures were done identically to the polycentric active zone tests. The results at 30 degrees are presented in Figure 30 to show the behavior of the hinge mechanism.

As with the polycentric mechanism testing, the unicentric active zone moment data can be plotted against each other to yield a visual relationship between spring pretention and required moment to displace the tibia. This is shown graphically in Figure 31. These results can be seen in tabular form in Table 3.

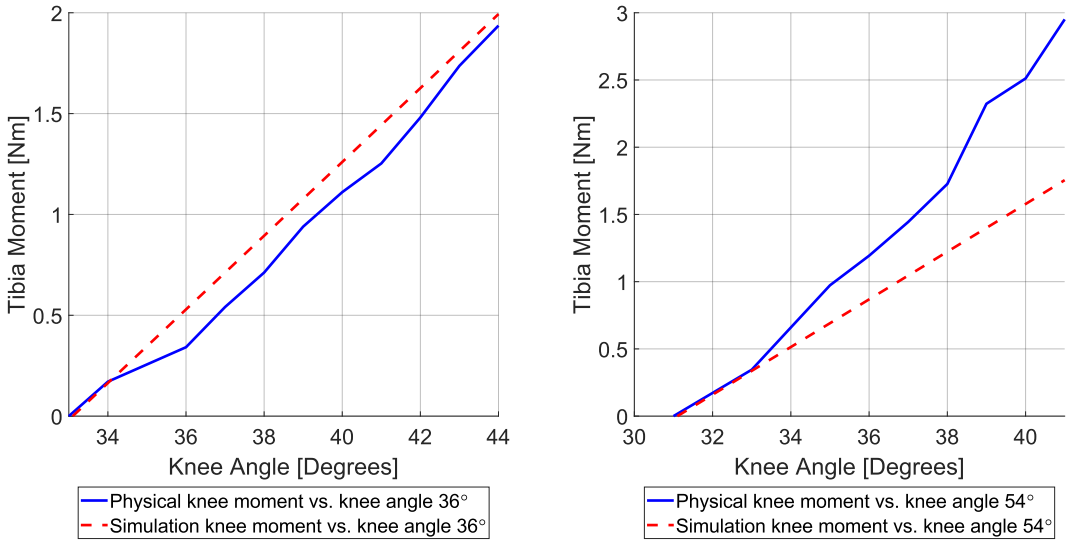

Figure 30: Active zone force requirements: 36 (left) and 54 (right) degree spring pretension, 30 degree knee angle, unicentric mechanism

	30 degree KA		
	Peak stiffness at 36 pretension	Peak stiffness at 54 pretension	Difference (%)
Simulated	1.993	1.755	12.716
Actual	1.936	2.951	41.524

Table 3: Differences between peak stiffness values at 36 and 54 degrees of spring pretension. Unicentric, 30 degree knee angle.

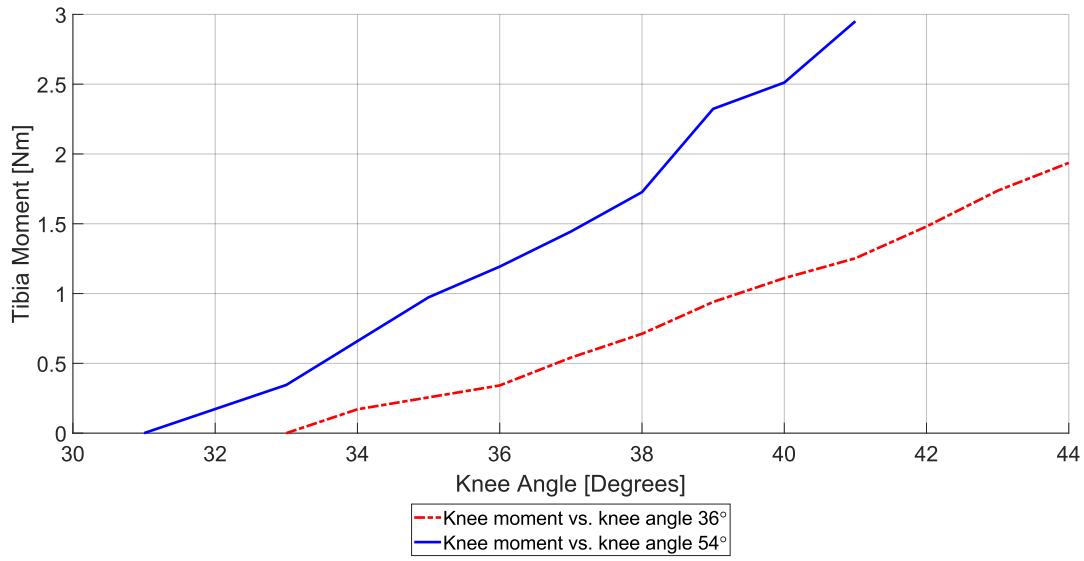

Figure 31: Comparison between pretension amounts at 30 degree knee angle, unicentric mechanism

4.3 Single-sided tests

Single-sided tests were performed using only one of the two springs to work against the direction of movement. This would be analogous, in a lower-body biomechanical sense, to using only the hamstring muscle to resist extension movement of the tibia or using only

the quadricep muscle to resist flexion movement of the tibia. First, the tibia was moved into a desired position for testing. Next, either the extension or flexion spring was locked into place. The opposing spring was taped into its neutral position so it could provide no torque into the system. Then the tibia was deflected such that the locked spring would resist its deflection, and this amount of resistance was recorded. In extension tests, the tibia is being extended, therefore the flexion spring would be resisting movement. Likewise, in flexion tests, the tibia was flexed, and the extensor spring would be resisting movement.

4.3.1 Polycentric

To determine the effectiveness of the spring-pulley-cam system at creating desired VSA behavior, tests were performed to determine the relationship between spring input angle and resultant stiffness of the tibial component. A code written in Matlab that uses only the spring deflections and linear spring stiffnesses was used as a comparison to the physical data. It is important to note that the simulation uses only the hypothetical stiffness of the knee joint derived from a stiffness equation given the spring displacement inputs. This is compared against physical testing data that comes from the resistance of the tibia to being displaced a certain amount.

Figure 32 and Figure 33 are the results of comparing the physical data (blue) to the simulated data (dashed red). Note that for the extension test, as the tibia would be pulled into extension, the test begins at a higher degree of flexion than it ends. Therefore, the x-axis of the graph iterates backwards. This is done to show the similarity of all tests.

4.3.2 Unicentric

Unicentric testing took place in the same way as polycentric testing. The simulation of testing was able to accommodate for a uniaxial joint, so these tests could also be compared in the same way as the polycentric tests. The simulation was able to account for a unicentric knee mechanism was by fixing the COR of the knee joint, causing a decrease in the available moment arm to actuate the joint during motion (R_e and R_f in equation (4.2)). Figure 34 shows the results of the single-sided flexion test, meaning the knee joint was pulled from extension to flexion. The spring resisting this motion would be the extension spring, which acts to move the tibia in extension. Therefore, the single-sided test examines how the extension spring reacts to a uniaxial joint moving into flexion.

Figure 35 shows the results of the single-sided extension test, meaning the knee joint was pulled from flexion to extension. The spring resisting this motion would be the flexion spring, which acts to move the tibia in flexion. Therefore, the single-sided test examines how the flexion spring reacts to a uniaxial joint moving into extension.

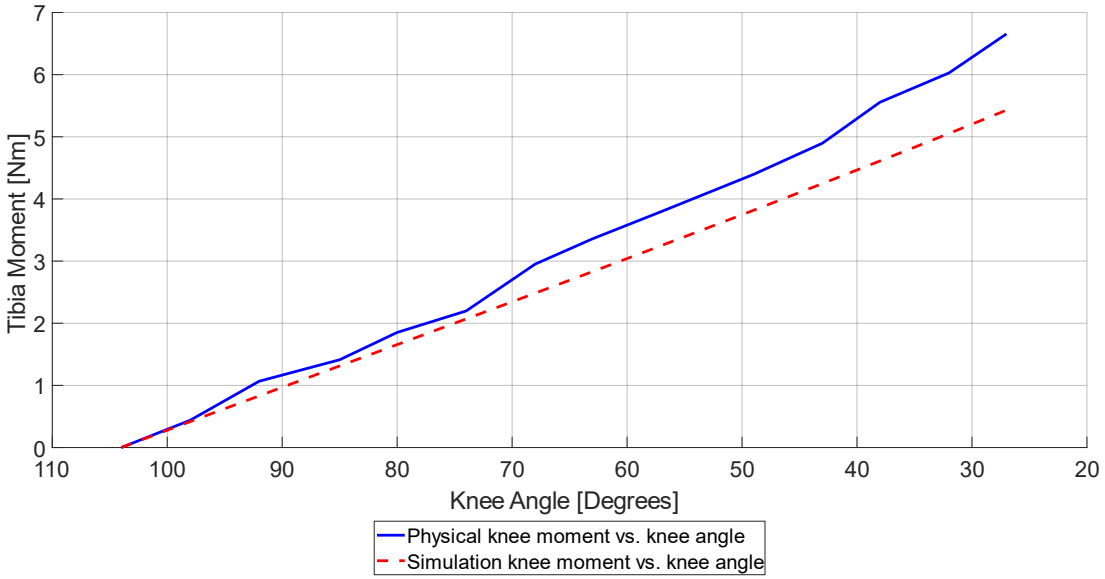

Figure 32: Single-sided polycentric extension test (testing flexion spring)

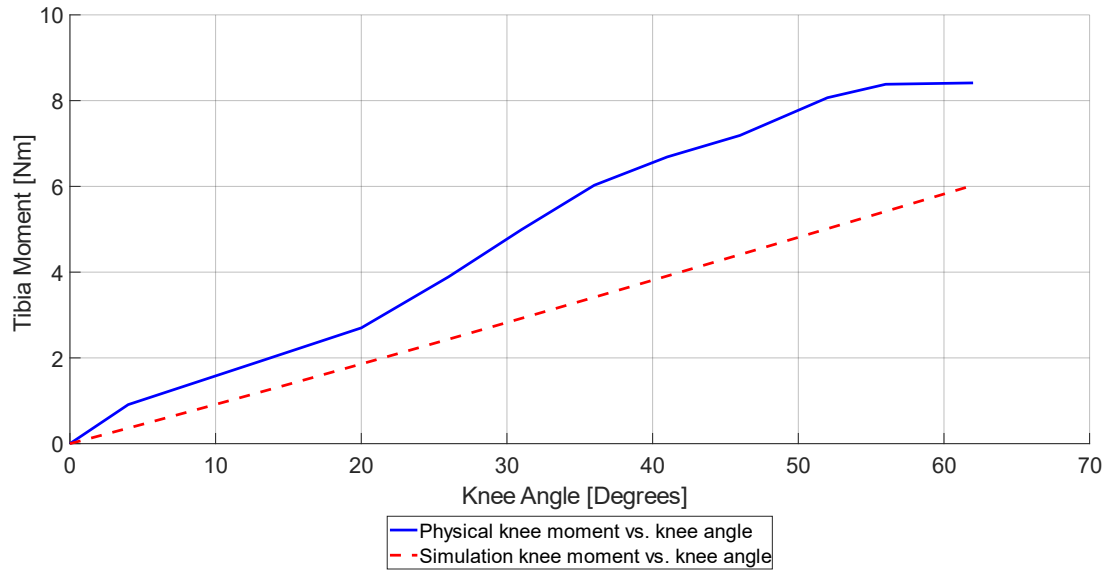

Figure 33: Single-sided polycentric flexion test (testing extension spring)

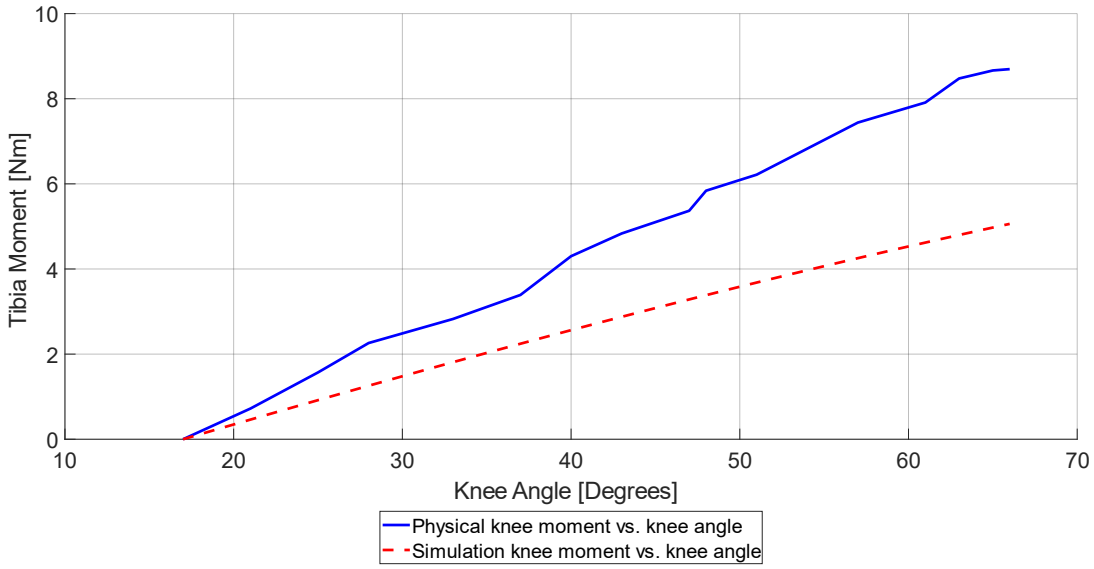

Figure 34: Single-sided unicentric flexion test (testing extension spring)

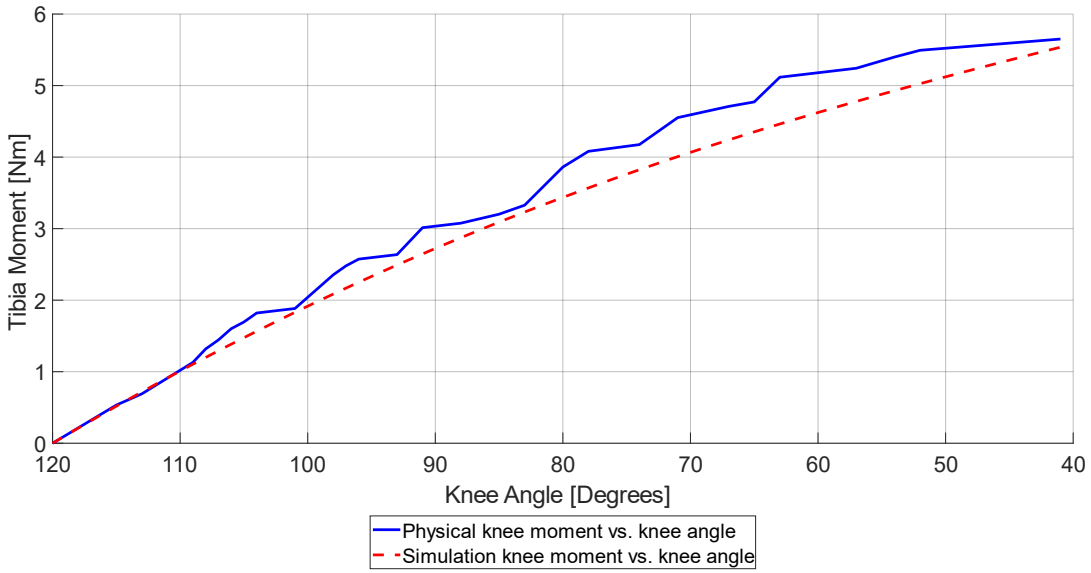

Figure 35: Single-sided unicentric extension test (testing flexion spring)

5. Discussion

This project, which has evolved over the course of its duration, will be summarized and discussed below. It is worth mentioning that the scope of the project has undergone significant shifts from its inception, leading to the validation testing performed in this work. The results shown In Section 4 and the proceeding discussion seek to quantify the feasibility of the design – *i.e*., the ability of this particular set of pulleys, cams, cables, and springs to control both the stiffness and position of the tibia.

5.1 Polycentric tests

The inception of the current work was centered around controlling a knee joint using the biologically inspired crossed four-bar geometry of the ACL-PCL complex. These rounds of testing, in essence, are the culmination of the work put into this project over the years. The desired results are a verification that the physical model and the simulation agree on the stiffening behavior of the knee joint during increased spring flexion. Agreement between the physical model and the simulation gives more confidence that simulations can yield correct results. This agreement will be discussed in further detail later in this document.

5.1.1 Physical vs. simulation

Two types of tests and subsequent simulation analysis were performed for the polycentric knee mechanism – the active zone tests and the single-sided tests. Looking first at the active zone tests Figure 27-Figure 31, it can be seen that at both 36 and 54 degrees of spring deflection, at both 30 and 60 degrees of knee flexion angle, the force required to displace

the end of the tibia matches very well with the simulation. Both rise as expected throughout the active region, as one spring is unloading, and one spring is loading based on the movement of the tibia. As one would expect, the amount of force required to displace the tibia increases from 36 degrees to 54 of bi-lateral pretension.

In all figures, the physical model increases above the simulated amount of torque required to displace the tibia. This is due to friction in the system, as not all rubbing parts could be eliminated completely from testing, however friction mitigation and clearance fits between parts were utilized when applicable. The physical data being higher than the simulated data is expected given the dis-inclusion of physical limitations to the simulation.

5.1.2 Standalone analysis

In a real environment, this would be analogous to setting the flexor and extensor springs to desired positions to yield a desired stiffness and knee angle, then testing the resistance of the knee to external movement. It would be expected that the more load that is placed into the springs, the stiffer the knee joint will become. This needed to be verified, as simply tightening two antagonistic springs does not necessarily create a mechanism that can control both stiffness and position. The ability to control both stiffness and position comes from the decoupling of force and displacement in the governing equations of motion, which is done typically by introducing a non-linear spring to have a nonlinearity inherent in the force output of the spring. In this case, linear springs can be used as the nonlinearity in this design comes from the variable moment arm provided by the cam pulley complex. This

variable moment arm is assisted by the fact that by using the four-bar mechanism to guide movement, the moment arm is increased by COR movement during flexion.

One advantage of the four-bar mechanism is the inherent stability of flexion. By having two attachments on both the femur and tibia, both connected by rigid links, the mechanism has more inherent stability about the long axis of the tibia. This is opposed to the connection of the unicentric device, which is one point.

The polycentric device also leads to a further improvement that could be implemented into the prosthesis. The path of the COR is the vital feature of the four-bar guiding mechanism, so it could potentially be isolated.

5.2 Unicentric tests

5.2.1 Physical vs. simulation

The inclusion of a unicentric joint was an addition to the project during the creation of the physical model. When inputting to the simulation that the COR of the mechanism does not move (unicentric), the stiffening curves of the simulation change. This change could be beneficial, as it showed a stiffening behavior in regions where the polycentric knee mechanism (changing COR location) showed low ability to stiffen. Therefore, agreement between the physical testing and the unicentric simulations is also important in characterizing the ability of the knee mechanism to stiffen as a prosthesis should.

Two types of tests and subsequent simulation analysis were performed for the unicentric knee joint – the active zone tests and the single-sided tests. The first analysis will be done

for the active zone testing. Much like the polycentric tests above, the uniaxial joint showed a higher stiffness when the spring mechanisms were set to a higher degree of flexion.

5.2.3 Standalone analysis

Many conventional knee prostheses use a simple hinge knee to approximate the movement of the biological knee. For example, the Ottobock C-leg utilizes a hinge knee with its microprocessor and hydraulic dampening system. The elimination of the four-bar system would remove some degree of biological similarity, but it could be argued that this sacrifice would be acceptable for the sake of a more simplistic design. As well as being more of a simple construction, it was shown in the simulations that the unicentric knee joint would be able to stiffen in different ranges of knee flexion than the polycentric knee mechanism. This was analyzed, as it could be beneficial in the future of this project to understand for what ranges which type of tibio-femoral interface would be the most beneficial.

5.3 Outcome measures

The outcomes of this project were stated in Section 1.2. First, a physical device needed to be developed in order to physically test the design's ability to control stiffness and position. Second, the physical device and its results were to be compared against a simulation to verify that the simulation gives realistic data, and that the physical model is acting in an expected manner. As shown, both goals have been achieved.

The development of the physical model underwent extensive iterative design to create a model that could be used to control stiffness and position. The entire ROM of the biological knee was able to be rendered by the scale model, satisfying the first objective of Section

1.2. The spring-driven device, which is an analog for setting hypothetical spiral springs into the pulley wheels, was created (as described in Section 3.2) and was successfully able to create a variable amount of torque on its output shaft based on a customizable amount of spring pretension. This satisfies the second objective in Section 1.2. The testing apparatus, including the biologically accurate crossed four-bar linkage and cam-pulley-cable interface, was linked to the spring-driven device via the pulleys and was able to control the movement of the pulleys to adjust the tibial position. It was also able to create opposing torques on the pulleys based on initial spring pretension, rendering a higher knee stiffness. The testing apparatus was able to be evaluated at a number of knee positions and spring pretensions, *i.e.*, it was able to be tested with various inputs to the device and was able to output a range of knee stiffnesses throughout the knee's ROM. These tests can be seen in Section 4 and their results are summarized in Sections 5.1and 5. 2. This satisfies the final three points of Section 1.3.

5.4 Research synthesis

The given work requires care when discussing its place in the field of antagonistically driven VSA prostheses, as no motors were used in its testing or design. Therefore, comparisons to existing works becomes a challenge, as this work was primarily a proof-of-concept. There are aspects of this design, however, that are comparable to previous works. The main differentiating factor of this work as opposed to other VSA knee prosthesis designs is the usage of the mechanisms physical design to introduce non-linearity in the spring output force.

First, a comparison to the works performed by English and Russel [17] is natural. Their work clearly defined the concepts of antagonistic joint actuation and solidified that a nonlinear spring output is required to have control over both stiffness and position of an actuated joint. In the current work, the user acts as the motors actuating the springs and the physical design geometries act as the nonlinearity for the springs. English and Russel also highlight the importance of addressing the physical imitations of the springs (*i.e.* maximum/minimum spring deflection), which was an important factor in the current work. The limits of testing done in Section 4 were influenced by physical limitations of the spiral spring analog device.

In terms of stiffness control, there are multiple ways to create nonlinearity in a controllable system. The simplest way would be to use springs with a nonlinear force profile, such as in [39] and was recommended by English and Russel. However, the usage of linear springs and a clever physical design can also be used, as in the current work. Kizilhan *et. al.*[40] describes methods of using a variable transmission ratio between the actuated joint and the force input location, a method that is utilized in this work by the movement of the ICR during knee flexion/extension. Our method of transmission ratio adjustment allows for linear springs to be used in the current agonist-antagonist setup. Other methods of using linear springs and still outputting a nonlinear force profile involve more complicated spring setups, as described by Migliore *et. al.*[16].

Finally, there have been publications that are similar to the current work in terms of antagonistically driven VSA knee prostheses. The work done by Tagliabue *et. al.* [39] even

includes spiral springs in its antagonistic setup. The drawbacks of this setup, however, are the incredibly specialized springs needed to yield the desired results. The current work is able to use simple linear springs to yield the desired results, which in future iterations could be leveraged to reduce costs of production.

One of the crucial parts of the current work is the inclusion of intelligent mechanical design. By carefully specifying four-bar, cam surface, and pulley geometries, a large range of stiffnesses can be rendered throughout a user's ROM. The implications of future intelligent mechanical design could be as simple as increasing the lengths of the four-bar geometries based on end-user height, and as advanced as turning the pulleys themselves into cams to yield a higher tension on cables at given tibial deflections. The important synthesis of the current work is that the dis-inclusion of motors in testing is not to be seen as invalidating the proposed work to ever become a VSA driven prosthesis, but rather the intelligent design of the biologically inspired knee prosthesis itself can render a wide range of possibilities when used in conjunction with an agonist-antagonist VSA.

6. Conclusions and future work

6.1 Conclusions

As the culmination of work that has been progressing since undergraduate work began in the summer of 2018, the current work seeks to unify all ideas behind a biologically inspired knee prosthesis using an antagonistically driven variable stiffness actuator. The idea was to create a functioning knee prosthesis that used the concepts of variable stiffness actuation to mimic our body's quadricep and hamstring control of the knee. While a functional prosthesis did not result directly, a great deal of beneficial work has come from this project. It has been shown that stiffness of this mechanism can be controlled, to a degree, by the antagonistic linear springs that were used. It has been shown that the simulation provides accurate data, verified by the built physical model. It has been shown that a physical model can be made, and that in the future, the springs could be moved into the mechanism by way of a specially designed spiral spring set inside the pulley wheels.

Controllability of the mechanism was established in the proposal document as being able to control both the stiffness and position of the knee joint. Using the passive stiffness of the springs, when they are both the same in terms of pretension/deflection, they can move in a 1:1 manner in opposite directions to actuate the joint. If the mechanism had independent control of the pretension of the springs and the rotation of the pulley wheels, then it follows that this 1:1 movement of the pulleys should be able to actuate the joint at any stiffness. This was impossible to test with the current setup, as the pretension is set and locked at a particular angle relative to the pulley shafts. Actuating the springs, therefore

the pulleys that attach to the cable, in opposite directions with the same amount of deflection therefore yields the position control that was sought after. Further deflections of the springs yield more tension on the cables, yielding a higher stiffness of the joint. As this amount of stiffness was able to be controlled as an input to the device, it can be seen that stiffness control was also achieved.

The simulation that was built for this mechanism was based on pure mechanical principles and internal torques/distances. The geometry for the mechanism was based on the internal reference frame used for the simulation, so the distances for the moment calculations are the same. The verification that the simulation provides valid data is also critical to the project moving forward. If we have trust in the model, then tweaks and experiments to the simulation can be trusted and optimized to yield a more fine-tuned geometry. For example, the geometries of the pulleys and cams can be changed very easily in the simulation, but it may prove difficult to physically alter the pulley and cam radii instantaneously for testing. Finally, the construction of the physical model proves that a few different kinds of manufacturing can be used effectively for this project. Extensive use of 3D printing reveals a few points to this project. First, the femoral component does not come under much stress during benchtop testing. This means that for multiple iterations (for example, multiple variations of cam/pulley radii) a simple, low-fill 3D print can be used to analyze the resulting stiffening capabilities of the mechanism. Having access to a detailed CAD model with geometries derived from the simulated version also helps to ensure that during manufacturing, all geometries match. A major problem that the physical model had to overcome was that of friction. As a major part of this mechanism is the interface between

the cams and the cables that attach to the tibia, this interface had to be as frictionless as possible. This was an issue with the 3D printed parts but could be mitigated by attaching a near frictionless surface on the interface. More friction came from the pulley shafts, as they needed to be long enough to clear the four-bar portion of the mechanism to have enough room for the spring devices. The length of these shafts meant that they required substantial support, provided by means of 3D printed supports mounted to the vertical piece of extruded aluminum that runs the vertical length of the mechanism. Friction and supports are two components that future rounds of physical models will need to heavily consider and design for. A custom designed spiral spring will also be required for this model. The designing of this spring is beyond the scope of this project, as validation and conceptual verification have become the main goals. This was done by adapting a pragmatic approach to designing for control of stiffness and position. With more time, desired input/output characteristics could be determined for a custom spring that is constrained to fit within the mechanism. This would also give a more condensed look, and one that would be easier to implement into an actual prosthesis.

The idea behind this design is sound. This thesis opens the door for more development for a novel, antagonistically driven VSA prosthesis. The geometry of the device can be optimized and simulated, all without the need for unnecessary iterative design. The lessons from the physical building of this prototype can be used for further iterations, to reduce the effects from friction and ensure proper constraints are placed.

6.2 Future Work

The first round of progress in the future of this design will be incorporating the springs into the pulley wheels themselves. In this project, it was deemed unnecessary to custom design these springs as this work was mainly for proof-of-concept. Incorporating the springs into the pulley wheels has several advantages over an external spring drive system. First, this would give independent control to the tension placed on the pulley rods (the force placed on the cables) and the position of both pulleys. This is something that was unable to be done in the current setup. Secondly, it would substantially decrease the size of the mechanism. A major consideration and obstacle of this project was finding enough space around the mechanism to properly orient the springs and ensure their shafts are properly aligned to not cause unwanted stresses on the pulleys. With a compact design, the spring mechanisms are reduced to the size of the pulley and the only decision is where the motors to actuate the spring arbor would need to be placed.

This leads to the second round of progress that needs to take place for this project – the addition of motors. Ideally, the motors could be small enough that they could be in line with the pulley shafts and connected via a worm gear drive. These motors would need a control scheme that is able to recognize and adjust the stiffness of the knee joint on the fly – which would require specialized sensors to be placed on key parts of the mechanism.

Another round of progress that needs to be addressed is the optimization of the cam/pulley geometries. As the distance from the knee's (four-bar's) COR to the cable attachment is a key element in the ability of the spring mechanisms to stiffen the joint, it would be worth adjusting the cam and pulley radii to see what combination yields the highest amount of

stiffness variation. This could also be extended into a discussion of whether the cams need to be perfectly circular in perimeter, or if an optimized non-circular cam shape based on knee angle and required stiffness could be explored.

Bibliography

[1] S. Au and H. Herr, "Powered ankle-foot prosthesis," *IEEE Robot. Autom. Mag.*, vol. 15, no. 3, pp. 52–59, Sep. 2008, doi: 10.1109/MRA.2008.927697.

[2] E. C. Martinez- Villalpando, J. Weber, G. Elliott, and H. Herr, "Design of an agonist-antagonist active knee prosthesis," in *2008 2nd IEEE RAS & EMBS International Conference on Biomedical Robotics and Biomechatronics*, Scottsdale, AZ, USA: IEEE, Oct. 2008, pp. 529–534. doi: 10.1109/BIOROB.2008.4762919.

[3] E. J. Rouse, L. M. Mooney, and H. M. Herr, "Clutchable series-elastic actuator: Implications for prosthetic knee design," *Int. J. Robot. Res.*, vol. 33, no. 13, pp. 1611–1625, Nov. 2014, doi: 10.1177/0278364914545673.

[4] C. Fanciullacci *et al.*, "Survey of transfemoral amputee experience and priorities for the user-centered design of powered robotic transfemoral prostheses," *J. NeuroEngineering Rehabil.*, vol. 18, no. 1, p. 168, Dec. 2021, doi: 10.1186/s12984-021-00944-x.

[5] R. Gailey, "Review of secondary physical conditions associated with lower-limb amputation and long-term prosthesis use," *J. Rehabil. Res. Dev.*, vol. 45, no. 1, pp. 15–30, Dec. 2008, doi: 10.1682/JRRD.2006.11.0147.

[6] R. Singh *et al.*, "Depression and anxiety symptoms after lower limb amputation: the rise and fall," *Clin. Rehabil.*, vol. 23, no. 3, pp. 281–286, Mar. 2009, doi: 10.1177/0269215508094710.

[7] R. R. Torrealba and E. D. Fonseca-Rojas, “Toward the Development of Knee Prostheses: Review of Current Active Devices,” *Appl. Mech. Rev.*, vol. 71, no. 030801, May 2019, doi: 10.1115/1.4043323.

[8] H. Liu, C. Chen, M. Hanson, R. Chaturvedi, S. Mattke, and R. Hillestad, *Economic Value of Advanced Transfemoral Prosthetics*. RAND Corporation, 2017. doi: 10.7249/RR2096.

[9] C. W. Radcliffe, “Four-bar linkage prosthetic knee mechanisms: Kinematics, alignment and prescription criteria,” *Prosthet. Orthot. Int.*, vol. 18, no. 3, pp. 159–173, Dec. 1994, doi: 10.3109/03093649409164401.

[10] D. Jin, R. Zhang, H. Dimo, R. Wang, and J. Zhang, “Kinematic and dynamic performance of prosthetic knee joint using six-bar mechanism,” *J. Rehabil. Res. Dev.*, vol. 40, no. 1, p. 39, 2003, doi: 10.1682/JRRD.2003.01.0039.

[11] J. T. Kahle, “Comparison of nonmicroprocessor knee mechanism versus C-Leg on Prosthesis Evaluation Questionnaire, stumbles, falls, walking tests, stair descent, and knee preference,” *J. Rehabil. Res. Dev.*, vol. 45, no. 1, pp. 1–14, Dec. 2008, doi: 10.1682/JRRD.2007.04.0054.

[12] A. Mohamed, A. Sexton, K. Simonsen, and C. A. McGibbon, “Development of a Mechanistic Hypothesis Linking Compensatory Biomechanics and Stepping Asymmetry during Gait of Transfemoral Amputees,” *Appl. Bionics Biomech.*, vol. 2019, pp. 1–15, Feb. 2019, doi: 10.1155/2019/4769242.

[13] A. B. Sawers and B. J. Hafner, “Outcomes associated with the use of microprocessor-controlled prosthetic knees among individuals with unilateral

transfemoral limb loss: A systematic review," *J. Rehabil. Res. Dev.*, vol. 50, no. 3, p. 273, 2013, doi: 10.1682/JRRD.2011.10.0187.

[14] C. A. McGibbon, D. E. Krebs, and M. S. Puniello, "Mechanical energy analysis identifies compensatory strategies in disabled elders' gait," *J. Biomech.*, vol. 34, no. 4, pp. 481–490, Apr. 2001, doi: 10.1016/S0021-9290(00)00220-7.

[15] K. F. Laurin-Kovitz, J. E. Colgate, and S. D. R. Carnes, "Design of components for programmable passive impedance," in *Proceedings. 1991 IEEE International Conference on Robotics and Automation*, Sacramento, CA, USA: IEEE Comput. Soc. Press, 1991, pp. 1476–1481. doi: 10.1109/ROBOT.1991.131824.

[16] S. A. Migliore, E. A. Brown, and S. P. DeWeerth, "Biologically Inspired Joint Stiffness Control," in *Proceedings of the 2005 IEEE International Conference on Robotics and Automation*, Barcelona, Spain: IEEE, 2005, pp. 4508–4513. doi: 10.1109/ROBOT.2005.1570814.

[17] C. E. English and D. Russell, "Mechanics and stiffness limitations of a variable stiffness actuator for use in prosthetic limbs," *Mech. Mach. Theory*, vol. 34, no. 1, pp. 7–25, Jan. 1999, doi: 10.1016/S0094-114X(98)00026-3.

[18] D. M. Daniel, W. H. . Akeson, and J. J. O'Connor, *Knee ligaments: structure, function, injury, and repair*. New York: Raven Press, 1990.

[19] J. J. O'Connor, T. L. Shercliff, E. Biden, and J. W. Goodfellow, "The Geometry of the Knee in the Sagittal Plane," *Proc. Inst. Mech. Eng. [H]*, vol. 203, no. 4, pp. 223–233, Dec. 1989, doi: 10.1243/PIME_PROC_1989_203_043_01.

[20] F. Flandry and G. Hommel, “Normal Anatomy and Biomechanics of the Knee,” *Sports Med. Arthrosc. Rev.*, vol. 19, no. 2, pp. 82–92, Jun. 2011, doi: 10.1097/JSA.0b013e318210c0aa.

[21] B. Innocenti, “Biomechanics: a fundamental tool with a long history (and even longer future!),” *Muscle Ligaments Tendons J.*, vol. 07, no. 04, p. 491, Jan. 2019, doi: 10.32098/mltj.04.2017.02.

[22] A. Kharb, V. Saini, Y. Jain, S. Dhiman, M. Tech, and Scholar, “A review of gait cycle and its parameters,” *IJCEM Int J Comput Eng Manag*, vol. 13, Jan. 2011.

[23] J. Bradley, D. FitzPatrick, D. Daniel, T. Shercliff, and J. O’Connor, “Orientation of the cruciate ligament in the sagittal plane. A method of predicting its length-change with flexion,” *J. Bone Joint Surg. Br.*, vol. 70-B, no. 1, pp. 94–99, Jan. 1988, doi: 10.1302/0301-620X.70B1.3339068.

[24] S. Wolf *et al.*, “Variable Stiffness Actuators: Review on Design and Components,” *IEEEASME Trans. Mechatron.*, vol. 21, no. 5, pp. 2418–2430, Oct. 2016, doi: 10.1109/TMECH.2015.2501019.

[25] J. Sun, Z. Guo, Y. Zhang, X. Xiao, and J. Tan, “A Novel Design of Serial Variable Stiffness Actuator Based on an Archimedean Spiral Relocation Mechanism,” *IEEEASME Trans. Mechatron.*, vol. 23, no. 5, pp. 2121–2131, Oct. 2018, doi: 10.1109/TMECH.2018.2854742.

[26] E. C. Martinez-Villalpando, L. Mooney, G. Elliott, and H. Herr, “Antagonistic active knee prosthesis. A metabolic cost of walking comparison with a variable-damping prosthetic knee,” in *2011 Annual International Conference of the IEEE*

Engineering in Medicine and Biology Society, Boston, MA: IEEE, Aug. 2011, pp. 8519–8522. doi: 10.1109/IEMBS.2011.6092102.

[27] C. A. McGibbon, S. Brandon, E. L. Bishop, C. Cowper-Smith, and E. N. Biden, "Biomechanical Study of a Tricompartmental Unloader Brace for Patellofemoral or Multicompartment Knee Osteoarthritis," *Front. Bioeng. Biotechnol.*, vol. 8, Jan. 2021, doi: 10.3389/fbioe.2020.604860.

[28] N. Hogan, "Adaptive stiffness control in human movement," *Adv. Bioeng.*, pp. 53–54, 1979.

[29] N. Hogan, "Impedance Control: An Approach to Manipulation: Part II—Implementation," *J. Dyn. Syst. Meas. Control*, vol. 107, no. 1, pp. 8–16, Mar. 1985, doi: 10.1115/1.3140713.

[30] G. A. Pratt and M. M. Williamson, "Series elastic actuators," in *Proceedings 1995 IEEE/RSJ International Conference on Intelligent Robots and Systems. Human Robot Interaction and Cooperative Robots*, Pittsburgh, PA, USA: IEEE Comput. Soc. Press, 1995, pp. 399–406. doi: 10.1109/IROS.1995.525827.

[31] J. Schuy, P. Beckerle, J. Wojtusch, S. Rinderknecht, and O. Von Stryk, "Conception and evaluation of a novel variable torsion stiffness for biomechanical applications," in *2012 4th IEEE RAS & EMBS International Conference on Biomedical Robotics and Biomechatronics (BioRob)*, Rome, Italy: IEEE, Jun. 2012, pp. 713–718. doi: 10.1109/BioRob.2012.6290778.

[32] E. J. Rouse, L. M. Mooney, E. C. Martinez-Villalpando, and H. M. Herr, "Clutchable series-elastic actuator: Design of a robotic knee prosthesis for minimum energy consumption," in *2013 IEEE 13th International Conference on Rehabilitation*

Robotics (ICORR), Seattle, WA: IEEE, Jun. 2013, pp. 1–6. doi: 10.1109/ICORR.2013.6650383.

[33] T. Shu, G. Herrera-Arcos, C. R. Taylor, and H. M. Herr, "Mechanoneural interfaces for bionic integration," *Nat. Rev. Bioeng.*, pp. 1–18, 2024.

[34] Z. Qaiser and S. Johnson, "Generalized Spiral Spring: A Bioinspired Tunable Stiffness Mechanism for Linear Response With High Resolution," *J. Mech. Robot.*, vol. 13, no. 1, p. 011007, Feb. 2021, doi: 10.1115/1.4045654.

[35] B. Vanderborght, N. G. Tsagarakis, C. Semini, R. Van Ham, and D. G. Caldwell, "MACCEPA 2.0: Adjustable compliant actuator with stiffening characteristic for energy efficient hopping," in *2009 IEEE International Conference on Robotics and Automation*, Kobe: IEEE, May 2009, pp. 544–549. doi: 10.1109/ROBOT.2009.5152204.

[36] T. Lenzi, M. Cempini, L. Hargrove, and T. Kuiken, "Design, development, and testing of a lightweight hybrid robotic knee prosthesis," *Int. J. Robot. Res.*, vol. 37, no. 8, pp. 953–976, Jul. 2018, doi: 10.1177/0278364918785993.

[37] G. R. Hunt, S. Hood, L. Gabert, and T. Lenzi, "Effect of Increasing Assistance From a Powered Prosthesis on Weight-Bearing Symmetry, Effort, and Speed During Stand-Up in Individuals With Above-Knee Amputation," *IEEE Trans. Neural Syst. Rehabil. Eng.*, vol. 31, pp. 11–21, 2023, doi: 10.1109/TNSRE.2022.3214806.

[38] C. Zhou, Z. Li, B. Hu, H. Zhan, and X. Han, "Analytical solution to bending and contact strength of spiral bevel gears in consideration of friction," *Int. J. Mech. Sci.*, vol. 128–129, pp. 475–485, Aug. 2017, doi: 10.1016/j.ijmecsci.2017.05.010.

[39] G. Tagliabue, V. Raveendranathan, A. Gariboldi, L. Y. Hut, A. Zucchelli, and R. Carloni, “MyKnee: Mechatronic Design of a Novel Powered Variable Stiffness Prosthetic Knee,” *IEEE Trans. Med. Robot. Bionics*, pp. 1–1, 2024, doi: 10.1109/TMRB.2024.3407194.

[40] H. Kizilhan, O. Baser, E. Kilic, and N. Ulusoy, “Comparison of Controllable Transmission Ratio Type Variable Stiffness Actuator with Antagonistic and Pre-tension Type Actuators for the Joints Exoskeleton Robots:,” in *Proceedings of the 12th International Conference on Informatics in Control, Automation and Robotics*, Colmar, Alsace, France: SCITEPRESS - Science and and Technology Publications, 2015, pp. 188–195. doi: 10.5220/0005507801880195.

Appendix A: Detailed Drawings

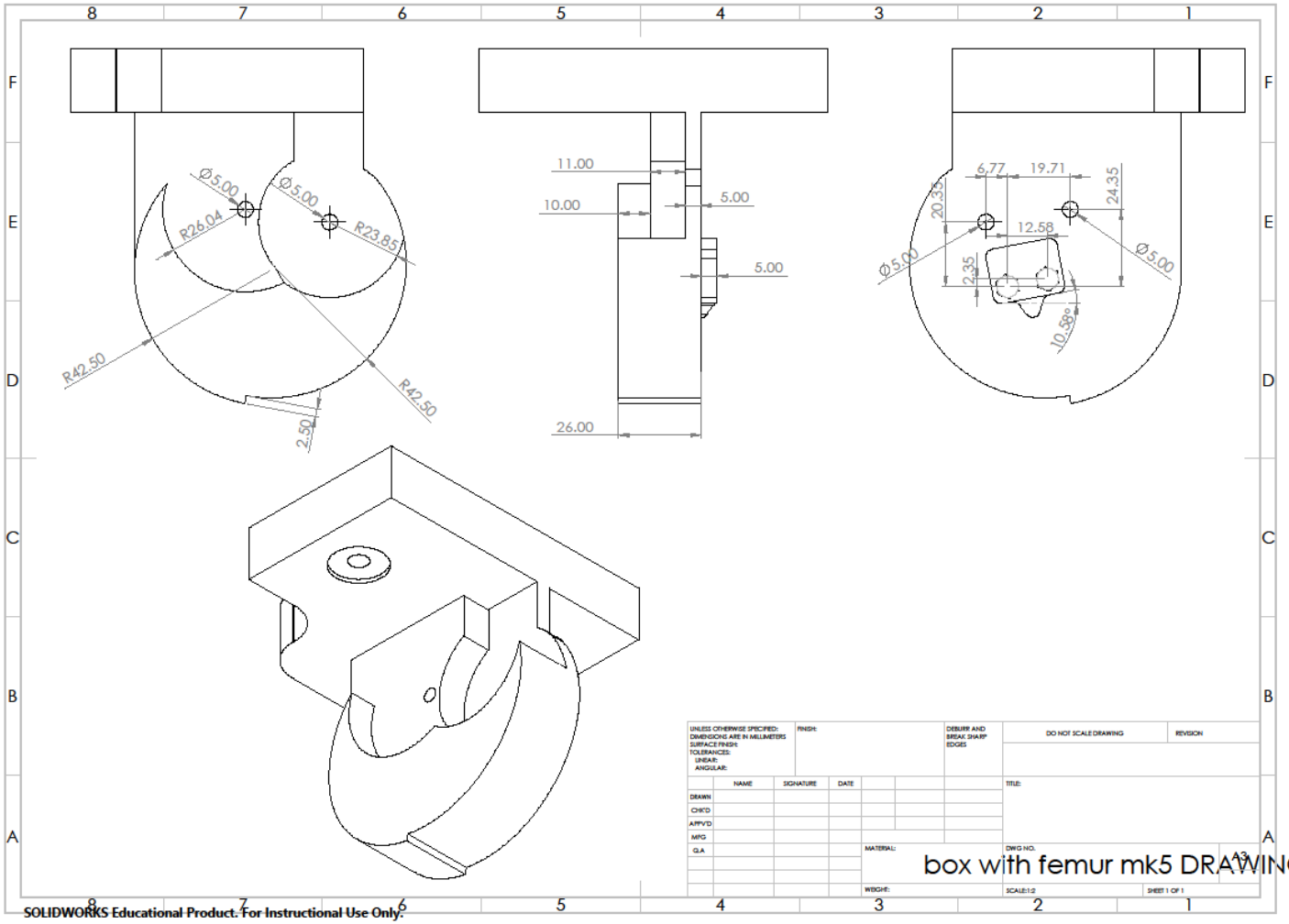

Figure 36: Detailed drawing of femoral component

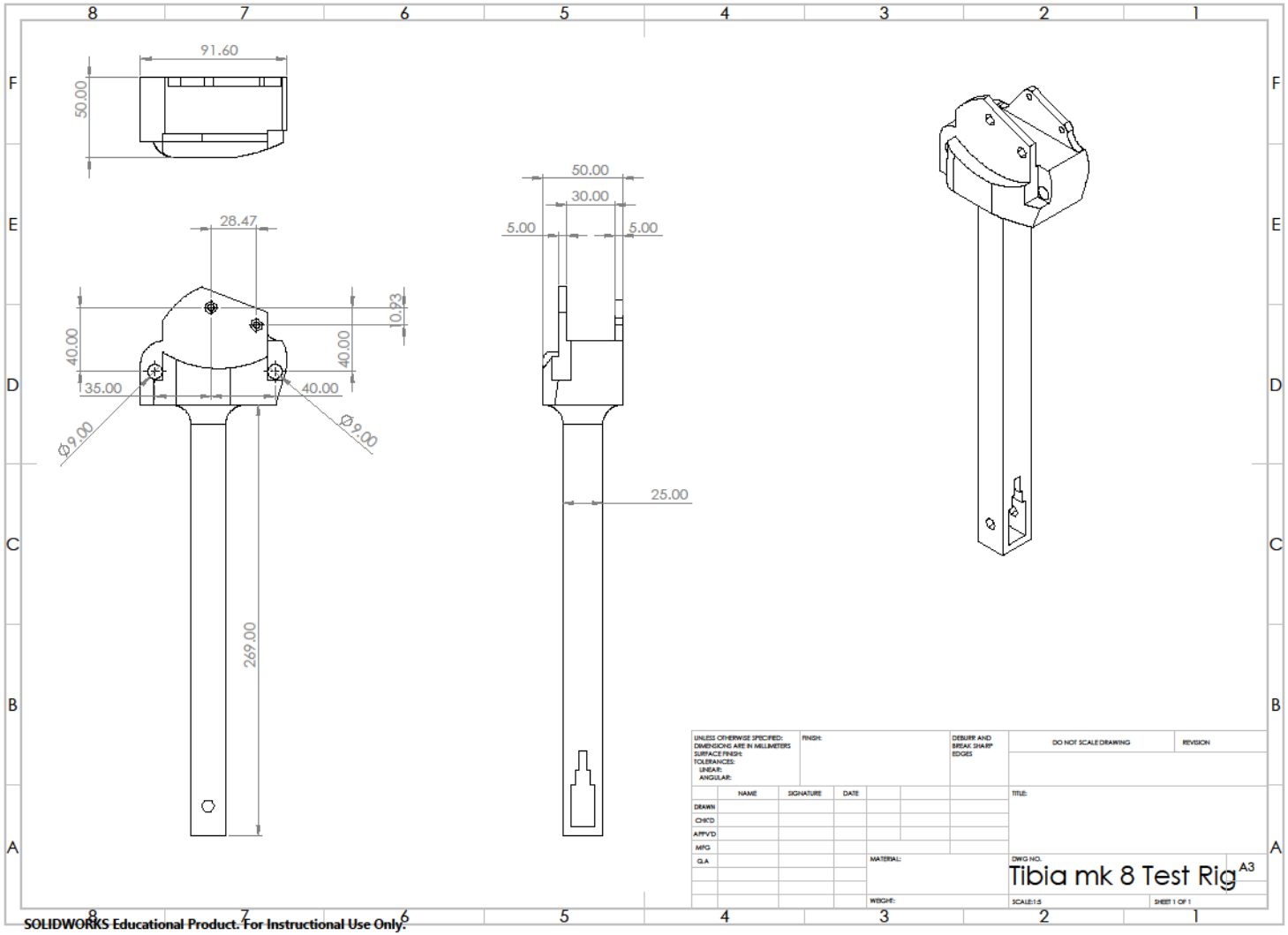

Figure 37: Detailed drawing of the tibial component

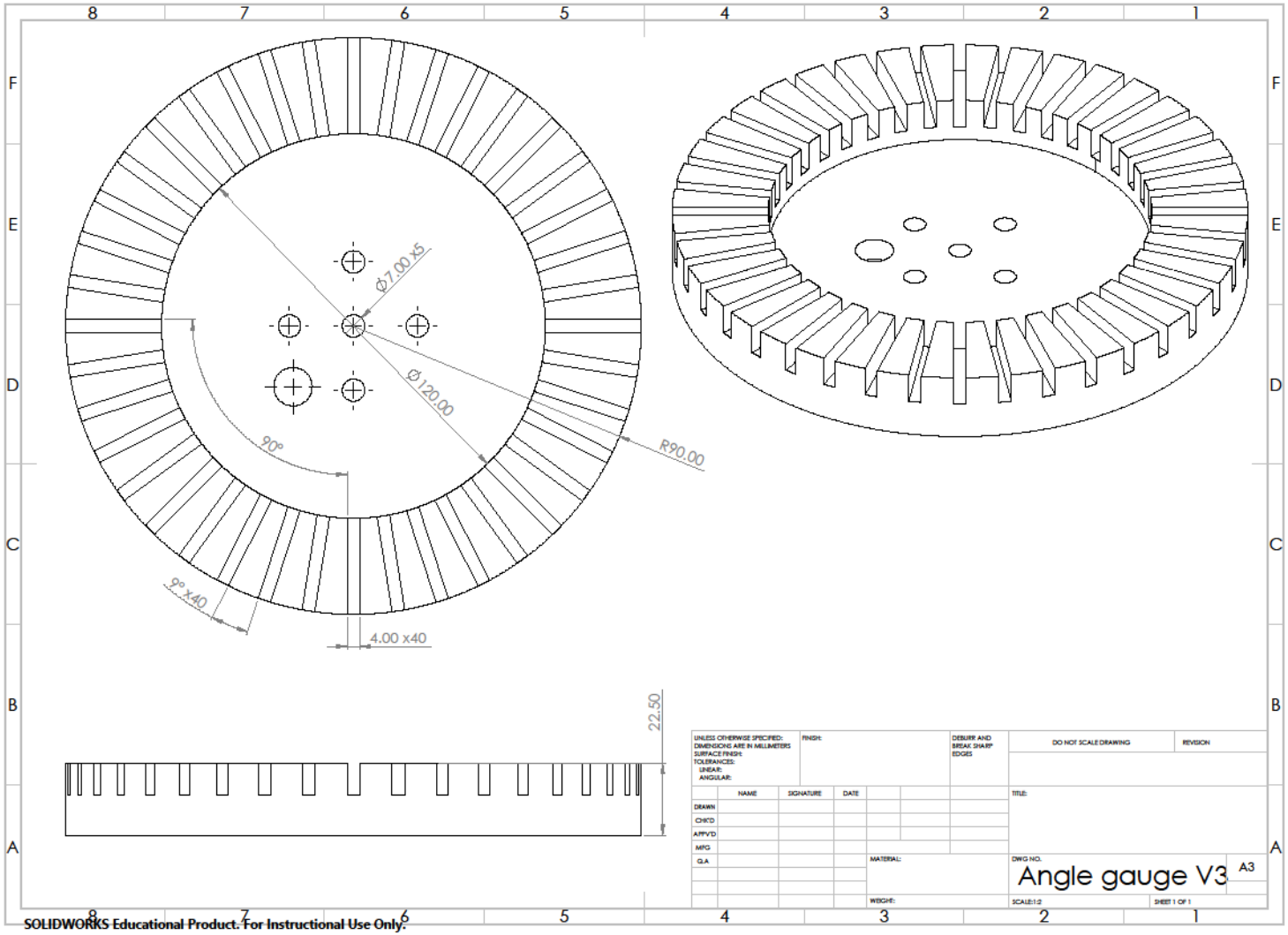

Figure 38: Detailed drawing of the angle gauge used in testing

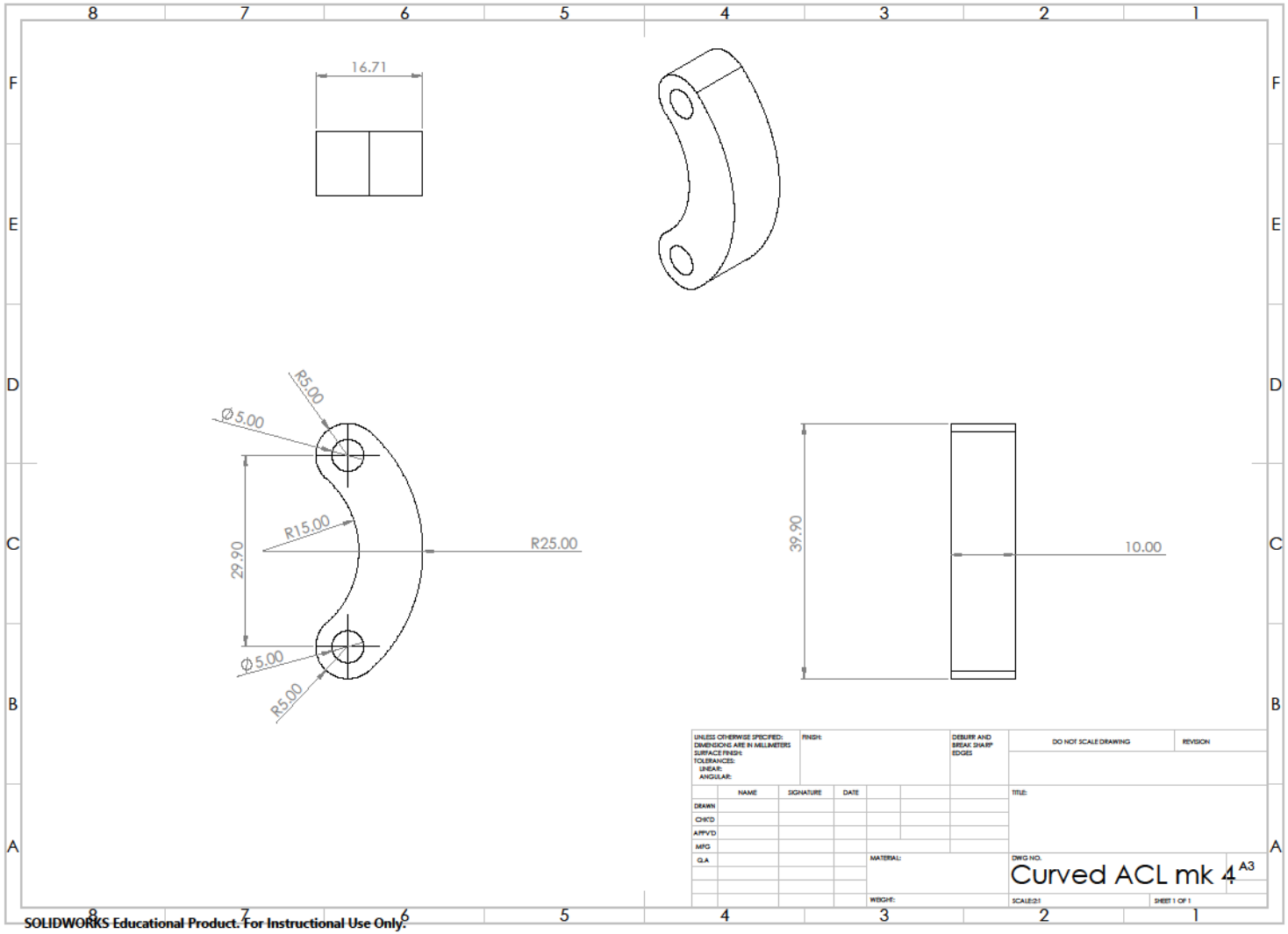

Figure 39: Detailed drawing of the ACL component

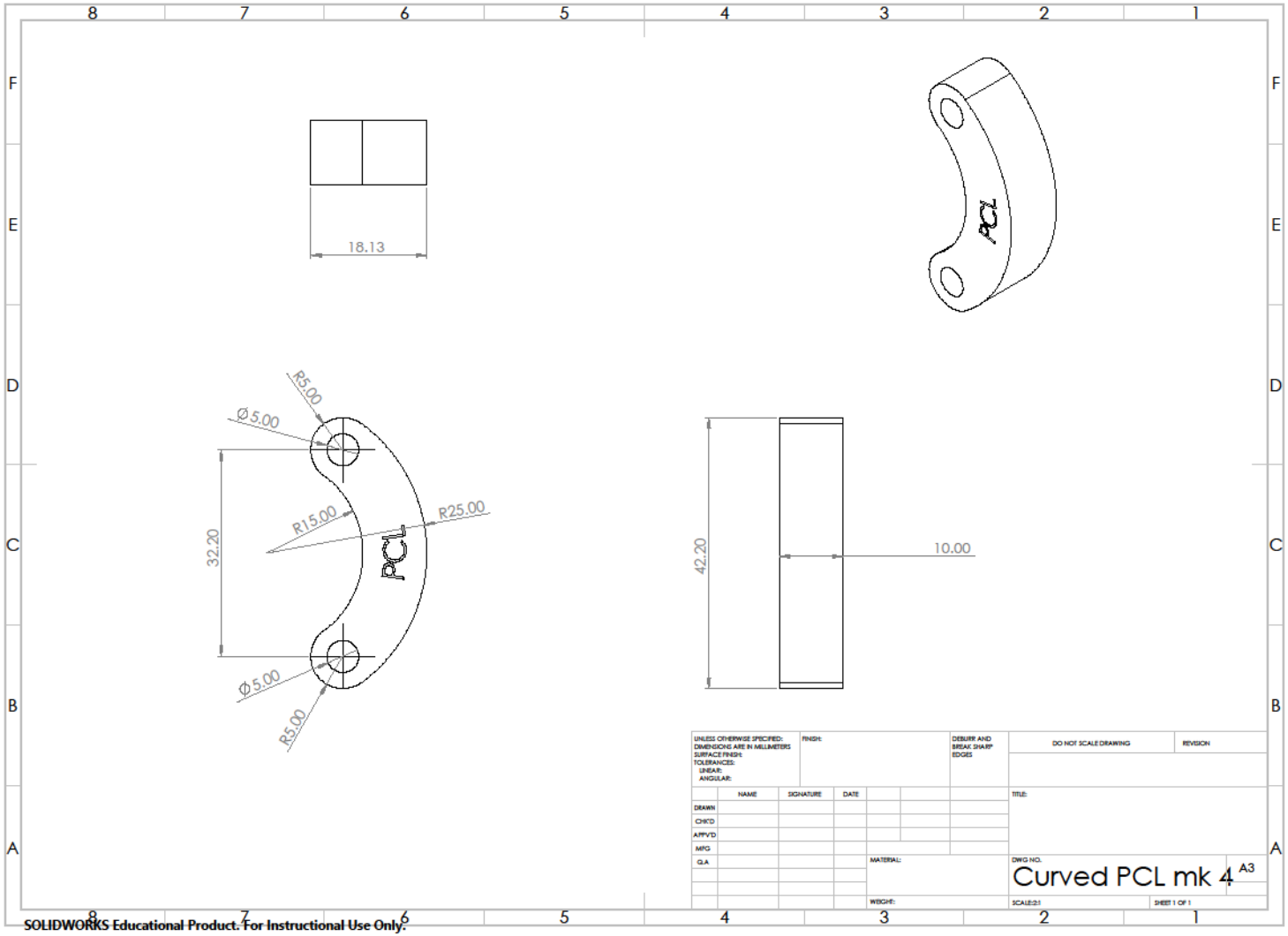

Figure 40: Detailed drawing of the ACL component

Appendix B: Design History

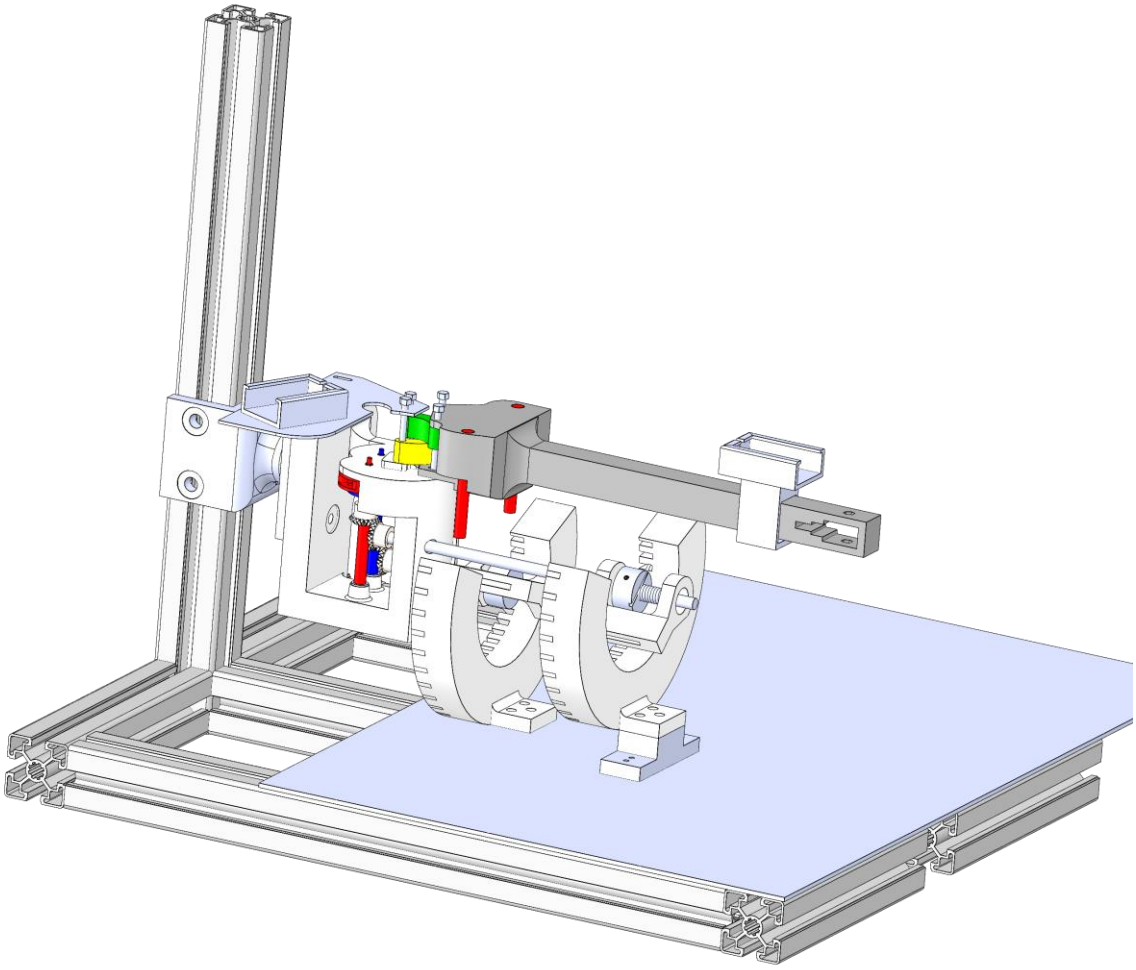

Figure 41: CAD model of prototype version 1

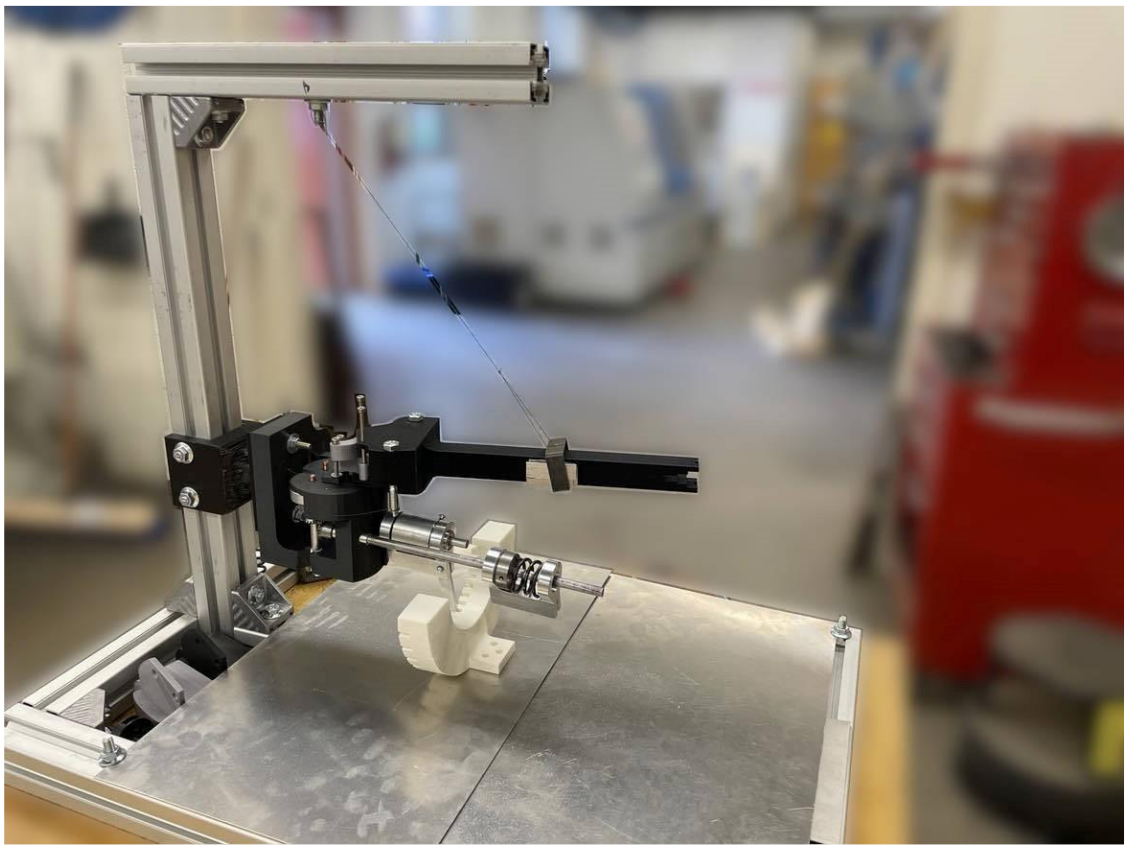

Figure 42: Physical model of prototype version 1

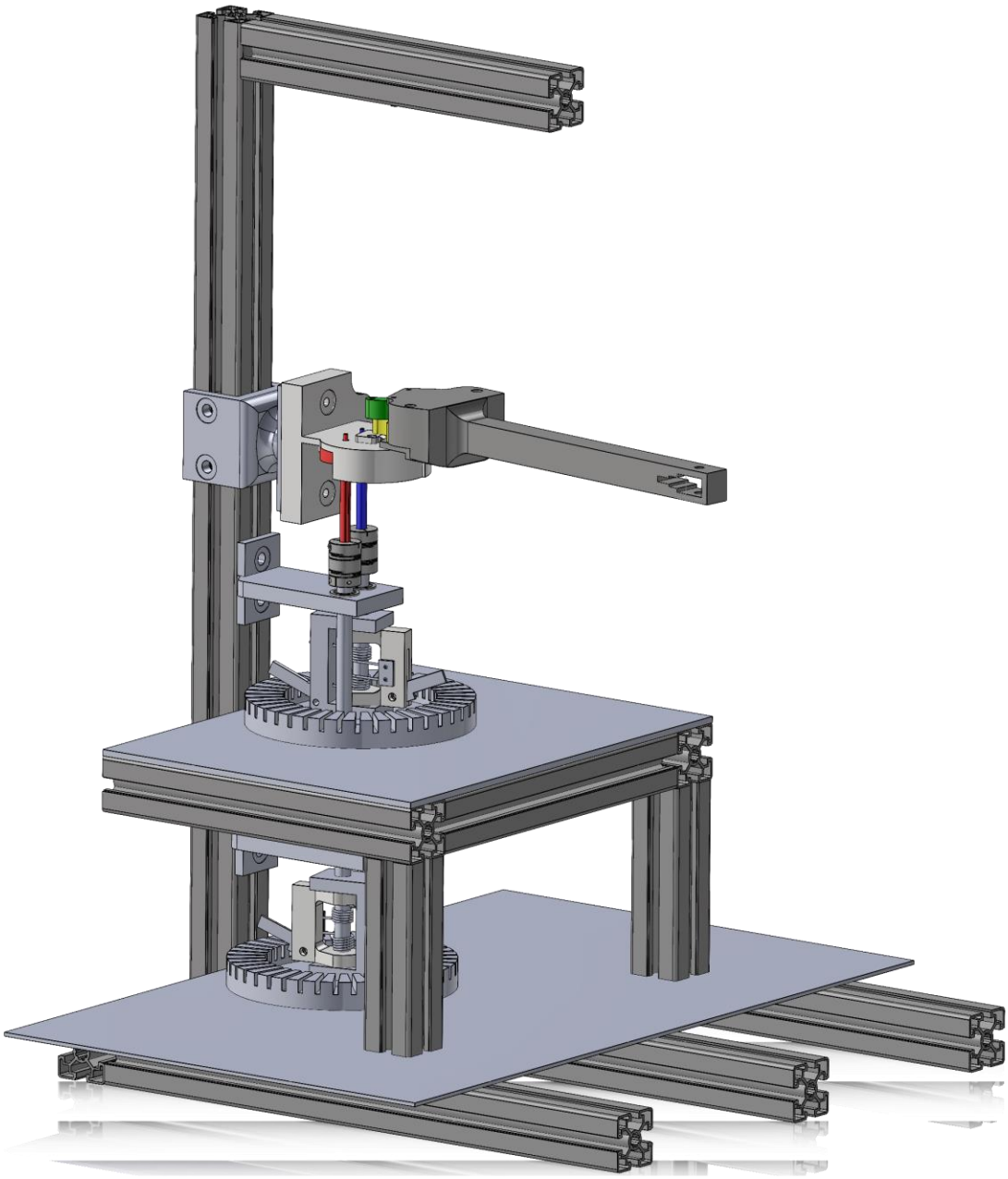

Figure 43: CAD model of prototype version 2

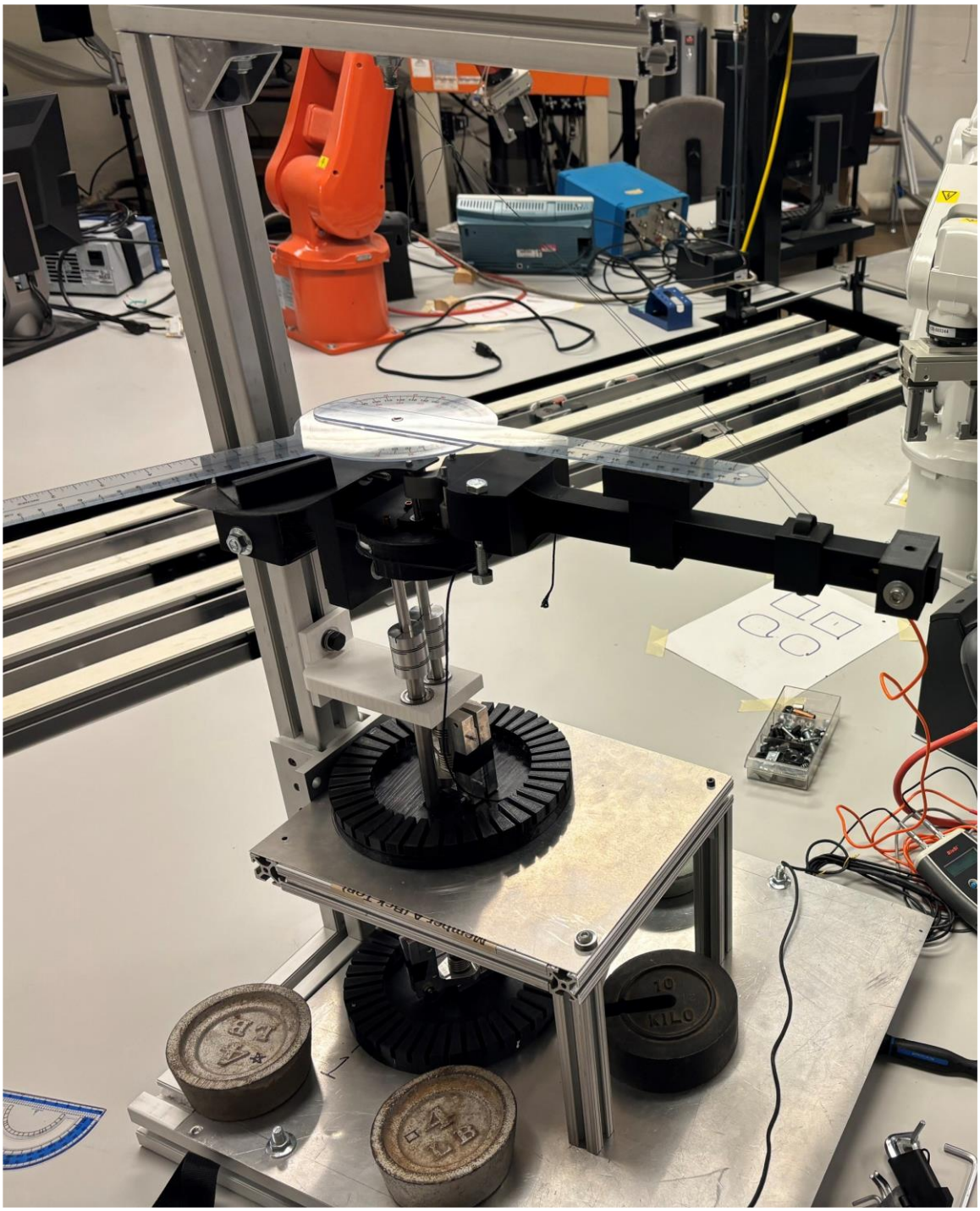

Figure 44: Physical model of prototype version 2

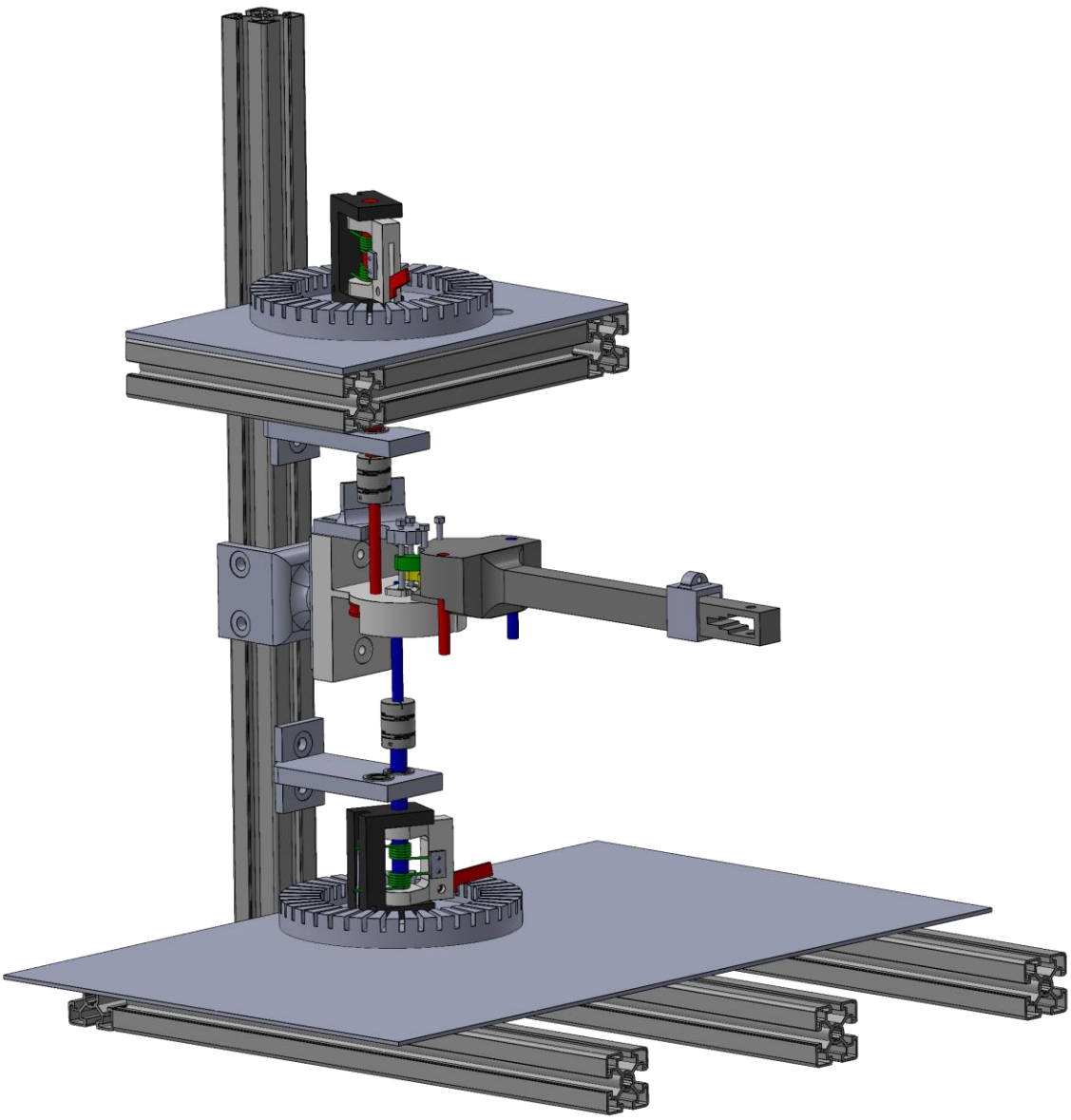

Figure 45: CAD model of prototype version 3 (final)

Figure 46: Physical model of prototype final version: whole model

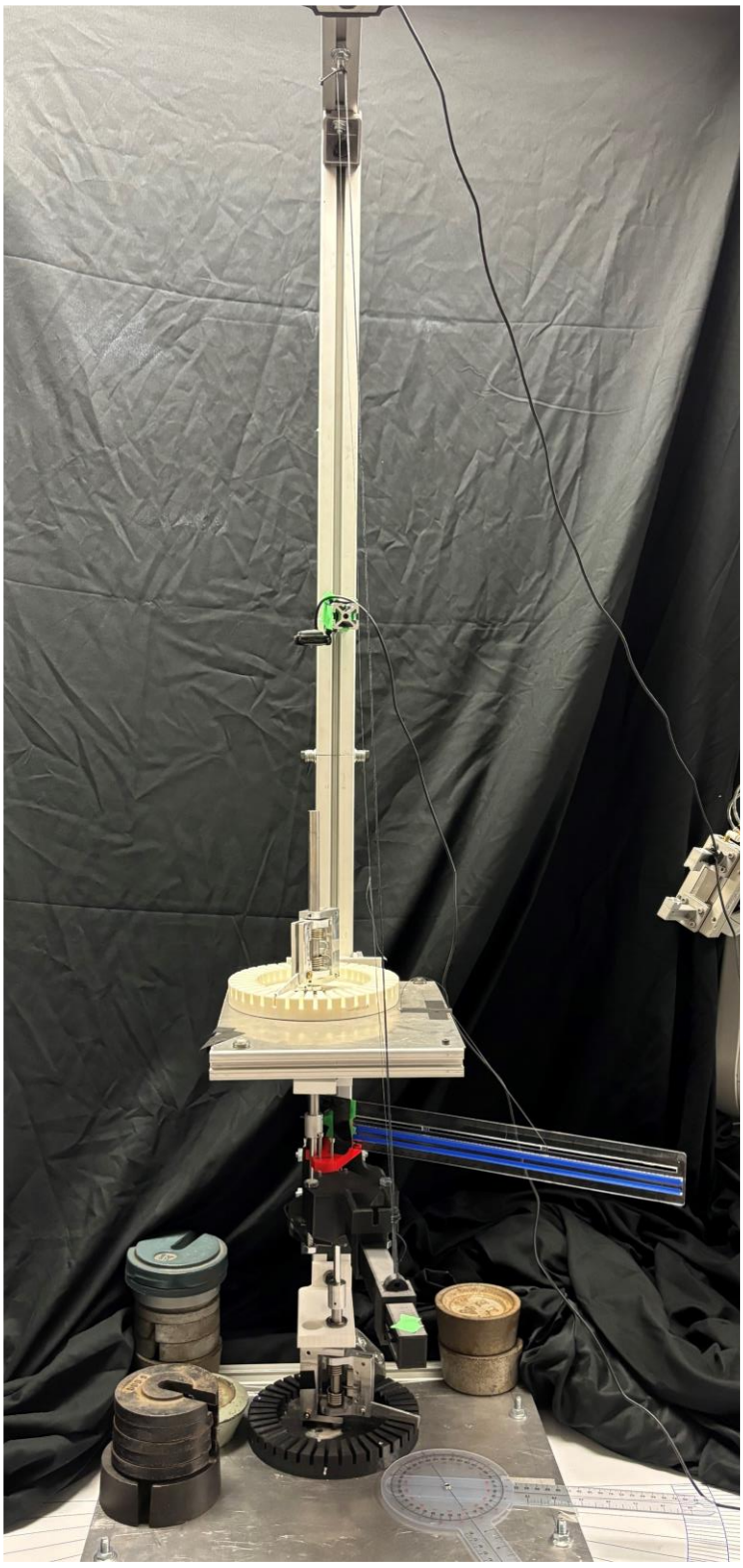

Figure 47: Physical model of prototype final version: front view

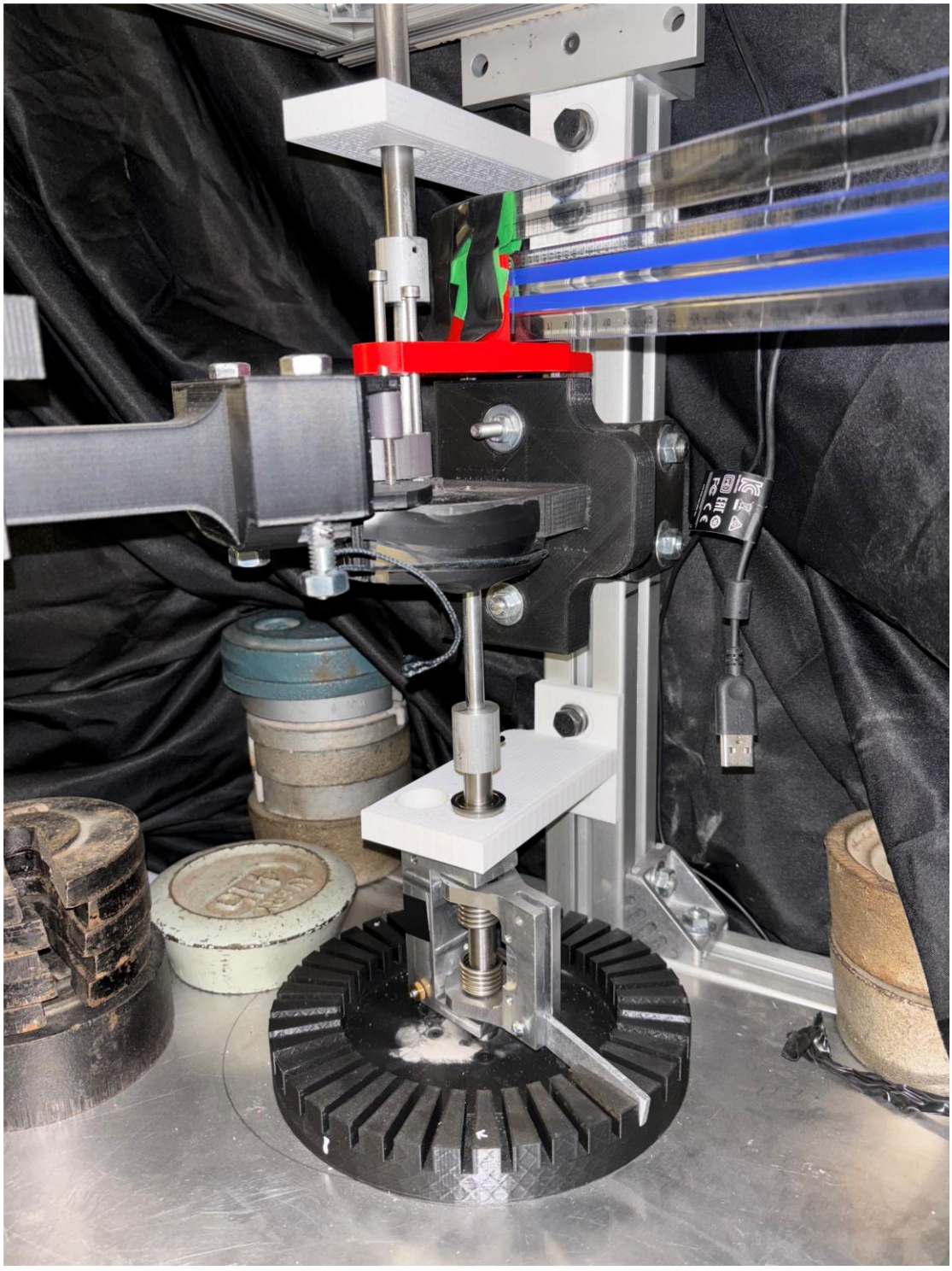

Figure 48: Physical model of prototype final version: middle detail

Appendix C: Luggage Scale Calibration Data

Test 1		
Weight [kg]	Scale Weight [kg]	Percent Error [%]
0.5	0.5	0
1	1	0
1.5	1.5	0
2	2	0
Weight [oz]	Scale Weight [oz]	Percent Error [%]
1	1	0
2	2	0
3	2	33.33
4	3	25
5	4	20
6	5.5	8.33
7	6.5	7.14
8	8	0
9	9	0
10	10	0
11	11.5	4.55
12	12	0
13	12.5	3.85
14	14	0
15	14.5	3.33
16	16	0

Table 4: Luggage scale calibration data, test 1

Test 2		
Weight [kg]	Scale Weight [kg]	Percent Error [%]
0.5	0.49	2
1	0.99	1
1.5	1.49	0.67
2	2.02	1
2.5	2.49	0.4
3	2.99	0.33
Weight [oz]	Scale Weight [oz]	Percent Error [%]
1	1	0
2	2	0
3	3.5	16.67
4	3	25
5	4	20
6	5.5	8.33
7	6.5	7.14
8	8	0
9	9	0
10	9.5	5
11	11	0
12	12	0
13	13	0
14	15	7.14
15	15	0
16	15.5	3.13

Table 5: Luggage scale calibration data, test 2

Curriculum Vitae

Candidate's full name:

Jacob Andrew Lufkin

Universities attended (with dates and degrees obtained):

B.Sc. Mechanical Engineering, University of New Brunswick, 2021

Publications: N/A

Conference Presentations:

"Towards Development and Prototyping of a Biologically Inspired Knee Prosthesis"

Jacob A. Lufkin, Chris A. McGibbon, Juan Antonio Carretero

2023 Canadian Committee for the Theory of Mechanisms and Machines (CCToMM)